AMERICAN SOCIETY FOR MICROBIOLOGY | mBio®

RESEARCH ARTICLE

Two Different Species of *Mycoplasma* Endosymbionts Can Influence *Trichomonas vaginalis* Pathophysiology

Valentina Margarita,[a] Nicholas P. Bailey,[b] Paola Rappelli,[a,c] Nicia Diaz,[a] Daniele Dessì,[a,c] Jennifer M. Fettweis,[d,e,f] Robert P. Hirt,[b] Pier Luigi Fiori[a,c]

[a]Department of Biomedical Sciences, University of Sassari, Sassari, Italy
[b]Biosciences Institute, Faculty of Medical Sciences, Newcastle University, Newcastle upon Tyne, United Kingdom
[c]Mediterranean Center for Disease Control (MCDC), Sassari, Italy
[d]Department of Microbiology and Immunology, School of Medicine, Virginia Commonwealth University, Richmond, Virginia, USA
[e]Department of Obstetrics and Gynecology, School of Medicine, Virginia Commonwealth University, Richmond, Virginia, USA
[f]Center for Microbiome Engineering and Data Analysis, Virginia Commonwealth University, Richmond, Virginia, USA

Valentina Margarita and Nick Bailey are co-first authors. Authors contributed equally to this work. Author order was determined in order of increasing seniority in this project.

ABSTRACT *Trichomonas vaginalis* can host the endosymbiont *Mycoplasma hominis*, an opportunistic pathogenic bacterium capable of modulating *T. vaginalis* pathobiology. Recently, a new noncultivable mycoplasma, "*Candidatus* Mycoplasma girerdii," has been shown to be closely associated with women affected by trichomoniasis, suggesting a biological association. Although several features of "*Ca.* M. girerdii" have been investigated through genomic analysis, the nature of the potential *T. vaginalis*-"*Ca.* M. girerdii" consortium and its impact on the biology and pathogenesis of both microorganisms have not yet been explored. Here, we investigate the association between "*Ca.* M. girerdii" and *T. vaginalis* isolated from patients affected by trichomoniasis, demonstrating their intracellular localization. By using an *in vitro* model system based on single- and double-*Mycoplasma* infection of *Mycoplasma*-free isogenic *T. vaginalis*, we investigated the ability of the protist to establish a relationship with the bacteria and impact *T. vaginalis* growth. Our data indicate likely competition between *M. hominis* and "*Ca.* M. girerdii" while infecting trichomonad cells. Comparative dual-transcriptomics data showed major shifts in parasite gene expression in response to the presence of *Mycoplasma*, including genes associated with energy metabolism and pathogenesis. Consistent with the transcriptomics data, both parasite-mediated hemolysis and binding to host epithelial cells were significantly upregulated in the presence of either *Mycoplasma* species. Taken together, these results support a model in which this microbial association could modulate the virulence of *T. vaginalis*.

IMPORTANCE *T. vaginalis* and *M. hominis* form a unique case of endosymbiosis that modulates the parasite's pathobiology. Recently, a new nonculturable mycoplasma species ("*Candidatus* Mycoplasma girerdii") has been described as closely associated with the protozoon. Here, we report the characterization of this endosymbiotic relationship. Clinical isolates of the parasite demonstrate that mycoplasmas are common among trichomoniasis patients. The relationships are studied by devising an *in vitro* system of single and/or double infections in isogenic protozoan recipients. Comparative growth experiments and transcriptomics data demonstrate that the composition of different microbial consortia influences the growth of the parasite and significantly modulates its transcriptomic profile, including metabolic enzymes and virulence genes such as adhesins and pore-forming proteins. The data on modulation from RNA sequencing (RNA-Seq) correlated closely with those of the cytopathic effect and adhesion to human target cells. We propose the hypothesis that the presence and the quantitative ratios of endosymbionts may contribute to modulating protozoan virulence. Our data highlight

Editor Patricia J. Johnson, University of California, Los Angeles

Address correspondence to Pier Luigi Fiori, fioripl@uniss.it, or Pier Luigi Hirt, robert.hirt@ncl.ac.uk.

The authors declare no conflict of interest.

Received 31 March 2022
Accepted 28 April 2022
Published 24 May 2022

the importance of considering pathogenic entities as microbial ecosystems, reinforcing the importance of the development of integrated diagnostic and therapeutic strategies.

KEYWORDS *Mycoplasma girerdii*, *Mycoplasma hominis*, pathogenicity, pathogroups, symbiosis, *Trichomonas vaginalis*, gene expression

Vaginal mucosal homeostasis requires an optimal combination of beneficial bacterial species, comprising a eubiotic microbiota, as well as host factors to minimize colonization opportunities for pathogenic microbes and maximize reproductive health (1). However, a complex combination of environmental factors, human genetics underlying innate and adaptive immune responses, and host physiology and behavior (2–4) can contribute to an imbalanced, dysbiotic microbiota. Dysbiosis is characterized by a highly dynamic vaginal microbial ecosystem that tends to increase the inflammatory tone of the mucosa, with diverse pathological consequences. Microbial dysbiosis contributes to pathologies of the urogenital tract, obstetric complications, and an increased risk of sexually transmitted infections such as HIV (5–7). One of the best-recognized and most common forms of vaginal dysbiosis among women of reproductive age has been defined as bacterial vaginosis (BV) (8). New -omics technologies have recently revealed that BV can be stratified into functionally different subtypes that are not resolved by more traditional diagnostic approaches (9). Most recent vaginal microbiome studies have used taxonomic surveys of the 16S rRNA gene and have thus surveyed only the bacterial composition of the microbiota. Microbial eukaryotes, including *Candida* species and *Trichomonas vaginalis*, can also contribute to dysbiosis in the vaginal microbial ecosystem, leading to a boost in the inflammatory tone of the vaginal tissues (10).

T. vaginalis is the causative agent of trichomoniasis, the most common nonviral sexually transmitted infection worldwide, which annually affects ~160 million men and women aged 15 to 49 years worldwide (11). Several studies have shown that *T. vaginalis* interaction with dysbiotic vaginal microbiota species qualitatively and quantitatively modulates the host inflammatory response, leading to pathogenesis. *T. vaginalis* is able to reduce the colonization of lactobacilli, which is associated with an increase in the number of anaerobic bacteria characteristic of BV, such as *Fannyhessea vaginae* (previously named *Atopobium vaginae*) (12), *Prevotella bivia*, *Megasphaera* sp., *Sneathia* sp., and *Gardnerella* sp. (13). More recently, *in vitro* models of polymicrobial infection revealed a correlation between *Fannyhessea* and *Gardnerella* species, two common BV-associated bacteria, alongside an enhancement of the pathogenic capabilities of *T. vaginalis* (14). The combination of these microbial pathogens in the vagina significantly affects the host immune response by boosting *T. vaginalis*-induced proinflammatory chemokine production and synergistically affecting the integrity of tight junctions between cervicovaginal epithelial cells, which together likely contribute to a reduction in mucosal barrier function *in vivo* (15, 16). The interplay between dysbiotic bacteria and *T. vaginalis* was further confirmed by Hinderfeld and Simoes-Barbosa, who demonstrated that biofilm produced *in vitro* by BV-associated bacteria is able to enhance the adhesion between protist and host cells, amplifying the parasite's cytopathic effect (14). Notably, *T. vaginalis* clinical isolates are able to carry *Mycoplasma hominis* (17), recently renamed *Metamycoplasma hominis* (18), an opportunistic pathogenic bacterium linked with pregnancy and postpartum complications, including spontaneous abortion, endometritis, and low birth weight (19). The interaction between *T. vaginalis* and *M. hominis* is the first endosymbiosis described between two obligate human mucosal parasites producing independent diseases in the same anatomical area (20).

The presence of *M. hominis* in *T. vaginalis* cells has been demonstrated in clinical isolates, with an association rate ranging from 5% to over 89% (21). Several studies have demonstrated how *M. hominis* associated with *T. vaginalis* influences the parasite's physiology and the dynamics of the host-parasite-bacterium interaction (22–25). More recently, a novel *Mycoplasma* species was characterized through 16S rRNA microbial surveys and metagenomic analyses. "*Candidatus* Mycoplasma girerdii," previously

referred to as "Mnola" (26) and recently renamed "*Candidatus* Malacoplasma girerdii" (18), shows an even tighter cooccurrence with *T. vaginalis* than *M. hominis*. The DNA of "*Ca.* M. girerdii" was detected almost exclusively in *T. vaginalis*-infected patients (26, 27). In addition to this specific association in the urogenital tract, 16S rRNA genes belonging to three *Mycoplasma* species, including *M. hominis* and "*Ca.* M. girerdii," were detected in the oral cavity of a premature neonate (28), and *T. vaginalis* and "*Ca.* M. girerdii" genomic DNAs (gDNAs) were also found to cooccur in a premature infant's saliva (29). In recent studies, sequences mapping to "*Ca.* M. girerdii" have been identified in several preterm birth cohorts of the vaginal microbiome (30–32), but given the low prevalence of the organism and the relatively small sample sizes of these studies, the association of "*Ca.* M. girerdii" with premature birth has yet to be adequately assessed. Notably, *T. vaginalis* infections are associated with several pregnancy and postpartum complications, including low birth weight, premature rupture of membranes, and preterm delivery (33). Notably, comorbidities are increasingly recognized to have important implications for diagnostics and treatment regimens during pregnancy (34). Hence, developing an understanding of the interactions between *T. vaginalis* and the two strongly associated *Mycoplasma* species will be essential for unraveling their respective contributions to adverse reproductive health outcomes. An improved understanding may also aid in the development of new approaches for treatment, including through nuanced modulation of the microbiota to regain vaginal eubiosis.

"*Ca.* M. girerdii" possesses typical *Mollicutes* features, such as a small genome (~619 kb), which reflects a limited metabolic capability and, thus, obligate dependence on its host as a source of essential metabolites (18). *In silico* reconstruction of metabolic pathways suggests that "*Ca.* M. girerdii" is glycolytic, similarly to *Mycoplasma genitalium*, and encodes all enzymes for the utilization of glucose as an energy source (27). In contrast, "*Ca.* M. girerdii" lacks gluconeogenesis, the tricarboxylic acid (TCA) cycle (Krebs cycle), and enzymes for purine, pyrimidine, and amino acid synthesis as well as the arginine dihydrolase (ADH) pathway, with the latter being essential for *M. hominis* energy metabolism (35). Notably, the "*Ca.* M. girerdii" genome also encodes proteins homologous to known microbial virulence factors, such as collagenase, hemolysin, and endopeptidase (27). A family of 26 genes encoding BspA-like proteins, containing *Treponema pallidum* leucine-rich repeat (TpLRR) domains (36), was also annotated in the genome of "*Ca.* M. girerdii" (27), and a larger family of genes encoding BspA-like proteins (911 members) was previously identified in *T. vaginalis* (37). Since some bacterial members of this protein family can stimulate a Toll-like receptor 2 (TLR2)-mediated host immune response (38), BspAs from various microbial sources may represent a common trigger of human inflammatory responses at various mucosal surfaces.

Predicted biological features of "*Ca.* M. girerdii" have been inferred through metagenomic analyses, and one very recent report supported the presumed symbiosis between *T. vaginalis* and "*Ca.* M. girerdii" (39). However, there are currently no data of relevance to the potential synergistic pathobiology of both microorganisms. In the current work, we provide the first molecular and mechanistic insights into this association, demonstrating that "*Ca.* M. girerdii" establishes an endosymbiotic relationship with the protist. Moreover, we present a new *in vitro* model in which isogenic mycoplasma-free *T. vaginalis* is infected with either "*Ca.* M. girerdii," *M. hominis*, or both mycoplasma species. This model system is used to investigate bacterial localization, multiplicity of infection (MOI), and the role of both *Mycoplasma* species in the modulation of *T. vaginalis* physiopathology.

RESULTS

Identification of "*Ca.* M. girerdii" and *M. hominis* and their MOIs in *T. vaginalis* clinical isolates. Analyzing the published 16S rRNA bacterial profiles of vaginal swabs (27) from 63 women diagnosed with trichomoniasis in more detail, we established that the majority (67%) of *T. vaginalis*-positive swabs (Real Time-PCR [RT-PCR] screening) were positive (≥0.1% 16S rRNA gene read count threshold) for either *M. hominis*, "*Ca.* M. girerdii," or both species (Table 1 and Fig. 1A and B). Similarly, the majority (83%) of 73 women with vaginal swabs positive for "*Ca.* M. girerdii" (≥0.1% 16S rRNA gene read

TABLE 1 Occurrence of *M. hominis* and "*Ca.* M. girerdii" among *T. vaginalis* isolates from vaginal swabs from trichomoniasis patients in Italy and 16S rRNA profiling of vaginal swabs from trichomoniasis patients in the United States

Isolate type	% of associated *T. vaginalis* strains[a] (no. associated/ total no. of isolates) (n = 75)	95% CI for no. of bacteria/ trichomonad cell (mean)[a]	% of associated 16S rRNA profiles of women with trichomoniasis[b] (no. associated/ total no. of isolates) (n = 63)
Mycoplasma-free *T. vaginalis*	11 (8/75)	0	33 (21/63)
T. vaginalis infected by "*Ca.* M. girerdii"	5 (4/75)	3.7–18.24 (10.97)	17 (11/63)
T. vaginalis infected by *M. hominis*	28 (21/75)	0.0001–5.6 (2.07)	22 (14/63)
T. vaginalis infected by "*Ca.* M. girerdii" and *M. hominis*	56 (42/75)	"*Ca.* M. girerdii," 0.003–0.1 (0.053) *M. hominis*, 0.001–39 (19.6)	27 (17/63)

[a]Parasite isolates derived from 75 vaginal swabs from patients with acute trichomoniasis from Italy (all Caucasian) were analyzed by qPCR for the presence of *M. hominis* and "*Ca.* M. girerdii." The percentage of strains associated with "*Ca.* M. girerdii" and/or *M. hominis* and the number of mycoplasma cells per *T. vaginalis* cell, evaluated by qPCR, are listed. The range and mean (in parentheses) MOI values are also listed. CI, confidence interval.

[b]16S rRNA microbiome profiles from vaginal swabs from 63 patients (87.3% Black American, 4.8% Caucasian, 3.2% Hispanic/Latino, and 3.2% unknown) with acute trichomoniasis were compared for the presence of *M. hominis* and "*Ca.* M. girerdii" (threshold of ≥0.1% of total 16S rRNA mapped reads).

count threshold) were also positive for *T. vaginalis* (RT-PCR) (Fig. 1C and D; see also Table S1 in the supplemental material).

Consistent with these bacterial taxonomic surveys of clinical samples, we also identified, by quantitative real-time PCR (qPCR), one or both *Mycoplasma* species of interest among the majority (89%) of clinical isolates of *T. vaginalis* grown in *in vitro* cultures (Table 1). Genomic DNA from 75 *T. vaginalis* isolates was analyzed by qPCR performed with *M. hominis*- and "*Ca*. M. girerdii"-specific primers, demonstrating the presence of *M. hominis* DNA in 63 strains and "*Ca*. M. girerdii" DNA in 46 strains. More than half of the strains harbored both *M. hominis* and "*Ca*. M. girerdii," whereas approximately one-third were positive for only *M. hominis* and a smaller fraction were positive for only "*Ca*. M. girerdii" (Table 1).

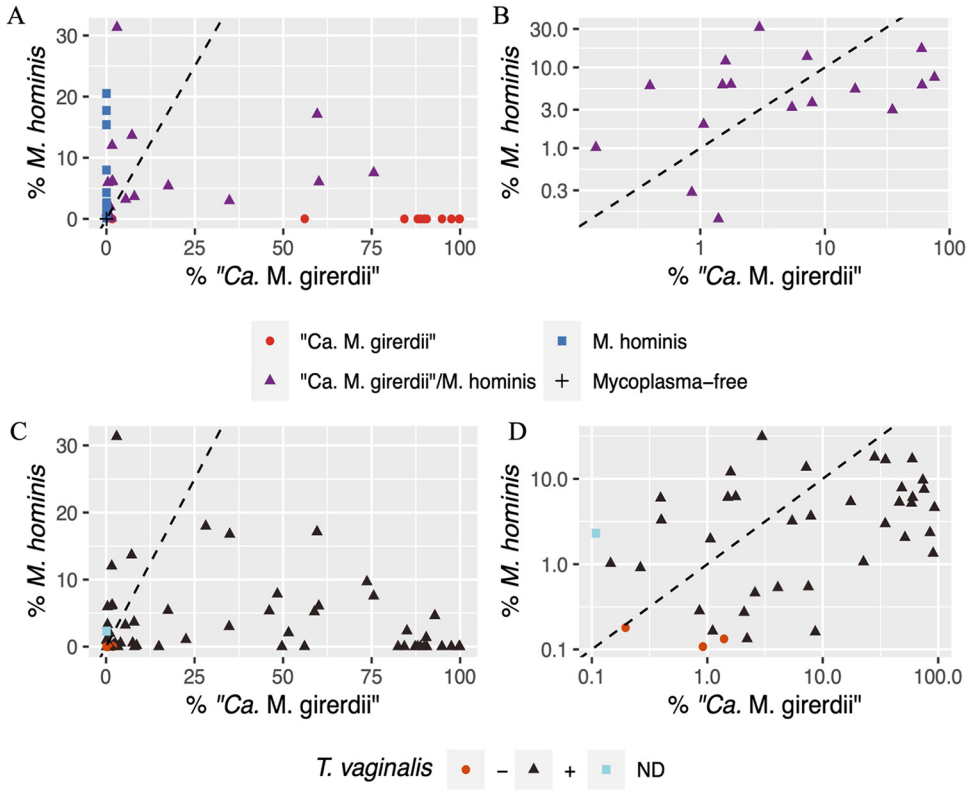

FIG 1 Proportion of 16S rRNA reads for "*Ca.* M. girerdii" and *M. hominis* from vaginal swabs from women either clinically diagnosed with trichomoniasis or positive for "*Ca.* M. girerdii." (A and B) Samples from 63 women clinically diagnosed with trichomoniasis. (C and D) Samples from 73 women with at least 0.1% of 16S rRNA reads mapped to "*Ca.* M. girerdii." ND, no data. Dashed lines indicate 1 to 1 ratio.

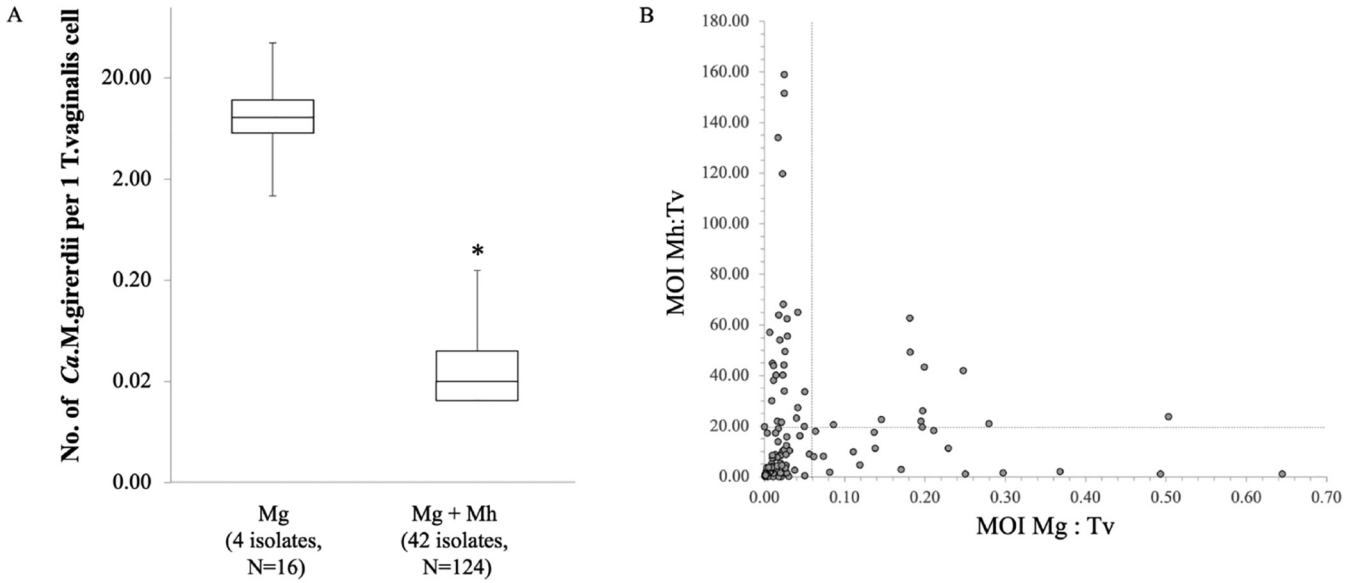

FIG 2 Multiplicity of infection of "*Ca.* M. girerdii" in *T. vaginalis* isolates. (A) Graph showing the variability in the number of bacteria per *T. vaginalis* cell among isolates associated exclusively with "*Ca.* M. girerdii" (Mg) and *T. vaginalis* strains dually infected by "*Ca.* M. girerdii" and *M. hominis* (Mg+Mh). Bars represent the means ± standard deviations (SD) from at least three independent growth experiments for each isolate of 2 isolates (Mg only) and 22 isolates (Mg+Mh), respectively. Statistical significance was tested by Student's *t* test, and * indicates significant ($P < 0.01$) variations in terms of the number of "*Ca.* M. girerdii" bacteria between parasites associated exclusively with "*Ca.* M. girerdii" and those in symbiosis with both *M. hominis* and "*Ca.* M. girerdii." (B) Plot area illustrating the relationship between the *M. hominis* MOI and the "*Ca.* M. girerdii" MOI in 22 dually infected *T. vaginalis* (Tv) strains. There are a total of 65 points corresponding to replicate cultures for the 22 dually infected strains. The negative trend observed among the 22 dual symbioses implies some form of direct competition between the two bacterial species. The horizontal dotted line indicates the mean value of the *M. hominis* MOI, while the vertical dotted line indicates the mean value of the MOI of "*Ca.* M. girerdii," among the 22 dually infected *T. vaginalis* clinical isolates.

Using qPCR, we investigated the MOIs of "*Ca.* M. girerdii" and *M. hominis* among different *T. vaginalis* isolates. The number of "*Ca.* M. girerdii" bacteria per trichomonad cell was evaluated, assuming that there is a single copy of the 16S rRNA gene present per genome, as shown previously for the four sequenced strains (27). Thus, one "*Ca.* M. girerdii" 16S rRNA copy corresponded to one "*Ca.* M. girerdii" cell. Differences in DNA extraction efficiency can impact the accuracy of MOI measures (40–42). In the absence of a cell wall, "*Ca.* M. girerdii" is predicted to be as easy to lyse as other mycoplasmas and *T. vaginalis*. Thus, we anticipate that differences in DNA extraction efficiencies would have a minimal impact on qPCR results. The evaluation of MOIs for *M. hominis* in *T. vaginalis* strains was carried out assuming that one copy of the MHO_0730 gene (GenBank accession number CAX37207.1) corresponded to one *M. hominis* cell, as shown for all 17 sequenced strains labeled as "complete genomes" and with fully conserved sequences for the sites targeted by the primers.

Using this approach, we observed that when "*Ca.* M. girerdii" was associated exclusively with *T. vaginalis*, the estimated mean MOI value was ~11 bacteria per *T. vaginalis* cell (Table 1). Notably, when both *M. hominis* and "*Ca.* M. girerdii" were present in the same *T. vaginalis* isolate, the "*Ca.* M. girerdii" MOI massively decreased from a ratio of ~11:1 to ~1:20 bacteria per *T. vaginalis* cell (Fig. 2A and Table 1). In contrast, the *M. hominis* MOI in symbiosis with *T. vaginalis* was 2:1, which increased to a mean value of ~20:1 in the context of dual symbiosis (Table 1).

These results indicate important isolate-to-isolate variability in the number of *M. hominis* and "*Ca.* M. girerdii" bacteria per *T. vaginalis* cell and that the presence of *M. hominis* has a significant impact on the ability of "*Ca.* M. girerdii" to grow within the parasite and vice versa. The inhibitory effect of the presence of *M. hominis* on the "*Ca.* M. girerdii" MOI among the 42 dual symbioses suggests direct competition between the bacterial species (Fig. 2B; Table S2). Furthermore, when comparing the 16S rRNA profiles of vaginal swabs (27), the proportion of reads mapping to "*Ca.* M. girerdii" or *M. hominis* 16S rRNA genes is also consistent with the two bacteria influencing each other (Fig. 1; Table S1).

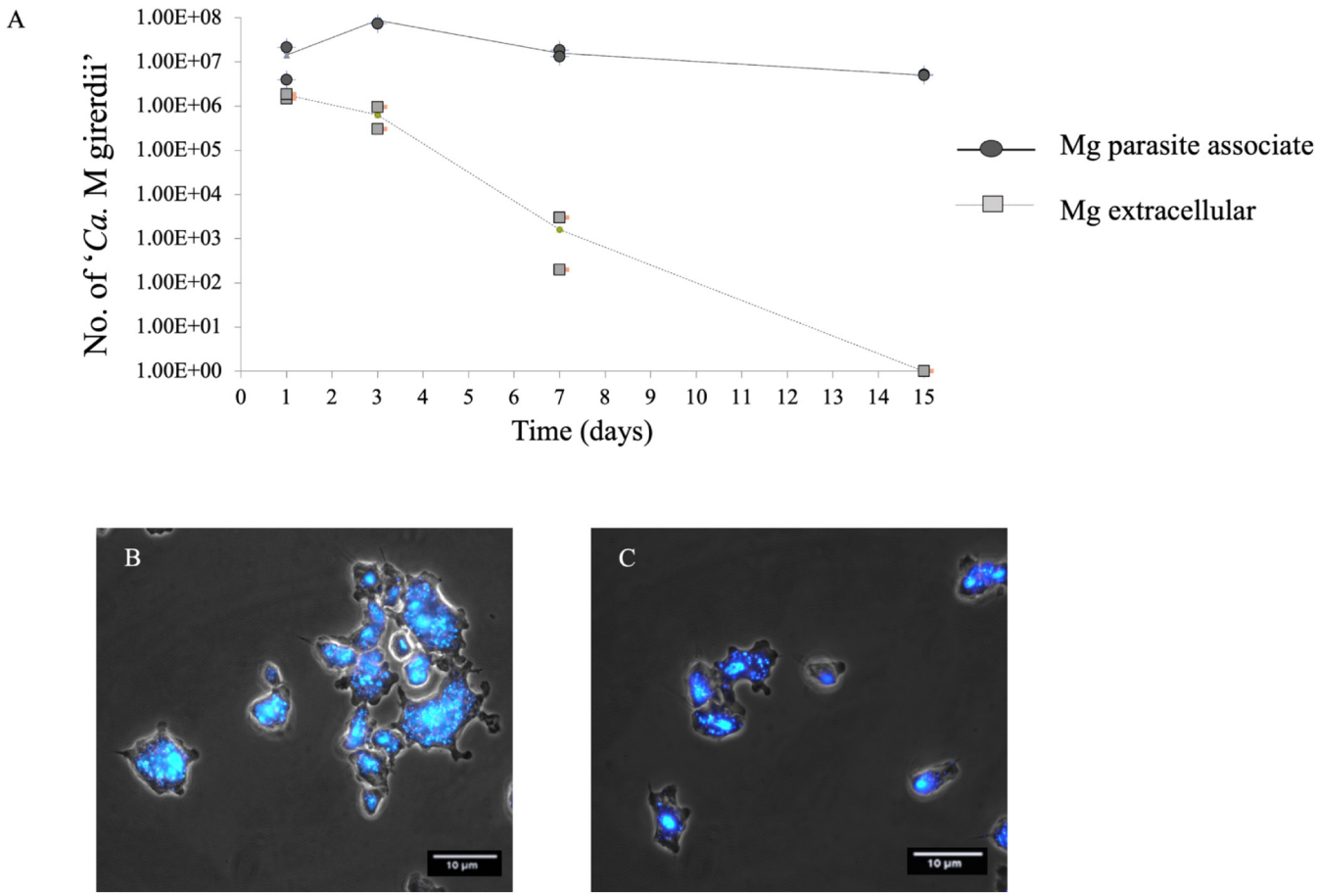

FIG 3 Effect of gentamicin treatment on "*Ca.* M. girerdii" associated with *T. vaginalis*. (A) TvSS-62Mg, a naturally "*Ca*. M. girerdii"-infected *T. vaginalis* isolate, was grown for 2 weeks in medium complemented with gentamicin in order to evaluate the susceptibility of the bacteria to the antibiotic treatment. Two replicate experiments were performed, and both data points are indicated. DNA from 1.00E+06 *T. vaginalis* cells/mL was extracted and analyzed by qPCR after 1, 3, 7, and 15 days of incubation with gentamicin. The curves refer to the number of "*Ca*. M. girerdii" bacteria found in association with the parasite (Mg parasite associate) and in the supernatant of cell cultures (extracellular) treated with gentamicin. The presence of live bacteria associated with *T. vaginalis* after up to 15 days of antibiotic treatment and their eventual disappearance after 15 days in the supernatant indicate that "*Ca.* M. girerdii" bacteria were able to multiply intracellularly, protected from the antibiotic. The intracellular persistence of "*Ca*. M. girerdii" in trichomonad cells after 15 days of gentamicin treatment was further supported by fluorescence (see panel C). (B) DAPI staining of TvSS-62Mg in the absence of exposure to gentamicin. (C) DAPI staining obtained following 2 weeks of antibiotic treatment of TvSS-62Mg cultures, indicating the presence of intracellular bacteria and consistent with the qPCR data illustrated in panel A.

Intracellular localization of "*Ca.* M. girerdii" in *T. vaginalis* cells: gentamicin protection and fluorescence assays. *T. vaginalis* strain SS-62 (TvSS-62Mg) was treated with gentamicin at a bactericidal concentration of 50 μg mL^{-1} in order to investigate whether "*Ca.* M. girerdii" is able to survive in the trichomonad cytoplasm, as the antibiotic does not enter the parasite (43–45). The susceptibility of "*Ca.* M. girerdii" to gentamicin was confirmed by the inability of gentamicin-treated supernatants to infect mycoplasma-free parasites. Aliquots were collected at days 1, 3, 7, and 15 during the gentamicin protection assay; subjected to total DNA extraction; and analyzed by qPCR to detect intracellular (*T. vaginalis* pellet) and extracellular (supernatant) "*Ca.* M. girerdii" DNA. As shown in Fig. 3A, "*Ca*. M. girerdii" DNA was detected in both trichomonad cells and the supernatant after up to 1 week of gentamicin treatment. Notably, after 15 days of cultivation in medium with gentamicin, "*Ca.* M. girerdii" DNA was still detected in *T. vaginalis* cells, while in contrast, it could not be detected in the corresponding supernatants of antibiotic-exposed cultures. The presence of bacteria in the parasite pellet demonstrates that they were able to survive the antibiotic treatment, thus suggesting an intracellular localization.

In order to further investigate the presence of "*Ca*. M. girerdii" in TvSS-62Mg after 2 weeks of cultivation in medium complemented with gentamicin, we performed a

fluorescence assay. Mycoplasma-associated parasites were stained using 4′,6-diamidino-2-phenylindole (DAPI) and analyzed by fluorescence microscopy. Figure 3B shows the clear presence of "*Ca.* M. girerdii" in the control *T. vaginalis* culture before treatment with the antibiotic, confirming the association between the parasite and mycoplasma under these *in vitro* culture conditions. Notably, Fig. 3C illustrates *T. vaginalis* cells still hosting intracellular "*Ca.* M. girerdii" after 15 days of cultivation in the presence of gentamicin, consistent with intracellular bacterial growth.

Ability of "*Ca.* M. girerdii" to infect *T. vaginalis* strains in the presence or absence of *M. hominis*. The ability of "*Ca.* M. girerdii" to establish a stable symbiotic relationship among *T. vaginalis* isolates in the presence or absence of *M. hominis* was studied *in vitro* using different parasite strains as recipients. In the first group of experiments, we coincubated the mycoplasma-free *T. vaginalis* reference strain G3 (TvG3) (46) with "*Ca.* M. girerdii" by using the same experimental strategy as the one described previously to infect *T. vaginalis* with *M. hominis* (24). The filtered supernatant of *T. vaginalis* isolate TvSS-62Mg, containing an average of 2.07E+06 "*Ca.* M. girerdii" bacteria, was added daily to a mid-log-phase culture of TvG3. The symbiosis between TvG3 and "*Ca.* M. girerdii" was confirmed by qPCR, showing the ability of this mycoplasma species to invade the parasite host (Fig. 4A). However, we noted that after ~10 freeze-thaw cycles during the storage of TvG3 in symbiosis with "*Ca.* M. girerdii" in liquid nitrogen, or following cultivation over longer periods (daily passages over 2 months), TvG3 could not maintain a stable association with "*Ca.* M. girerdii." In contrast, a number of *T. vaginalis* strains, including TvG3, are able to maintain a stable symbiotic relationship over time with *M. hominis* (47). These data suggest that when a mycoplasma-free *T. vaginalis* strain is used as a recipient, the *in vitro* symbiosis with "*Ca.* M. girerdii" is less stable than with *M. hominis*.

Due to the instability of the symbiosis between TvG3 and "*Ca.* M. girerdii," we studied the mycoplasma-parasite relationship using a different experimental approach. Two *T. vaginalis* strains, TvSS-25MgMh and TvSS-62Mg, naturally infected either by both *M. hominis* and "*Ca.* M. girerdii" or by "*Ca.* M. girerdii," respectively, were treated with Plasmocin (48), resulting in the corresponding axenic mycoplasma-free strains (TvSS-25iso and TvSS-62iso). TvSS-62iso and *T. vaginalis* strain G3, which is naturally *Mycoplasma* free, were cultivated for 30 days to evaluate the influence of treatment on trichomonad growth. As shown in Fig. S1A, the growth of TvSS-62iso is not significantly distinct from the growth of TvG3. Subsequently, TvSS-25iso and TvSS-62iso were used as recipients in order to produce *in vitro* single- and double-mycoplasma infections (Fig. 4B and C). This experimental model showed that "*Ca.* M. girerdii" is able to form a stable symbiosis with both trichomonad strains cultivated with daily passages over 15 days, suggesting that a previous adaptation to host mycoplasma, either *M. hominis* or "*Ca.* M. girerdii," can predispose a subsequent stable infection by "*Ca.* M. girerdii" under the conditions of these experiments. Notably, both *T. vaginalis* strains, when previously infected with "*Ca.* M. girerdii," can form a symbiosis with *M. hominis* but not vice versa, suggesting that symbiosis with *M. hominis* inhibits subsequent symbiosis with "*Ca.* M. girerdii," while the presence of "*Ca.* M. girerdii" does not block symbiosis with *M. hominis* under the tested conditions (Table 2).

The kinetics of infection obtained by comparing the MOI values of *Mycoplasma* in TvSS-62 and TvSS-62Mg+Mh confirmed the data from the clinical isolates: in the presence of a stable *M. hominis* infection, the number of "*Ca.* M. girerdii" bacteria associated with *T. vaginalis* decreases, compared with *T. vaginalis* associated with "*Ca.* M. girerdii" only (Fig. S1B).

The qPCR-based quantification data were further supported by a fluorescence assay. TvSS-62Mg can host a high number of bacteria (Fig. 5A) (mean MOI of 15:1). The absence of *M. hominis* in TvSS-62Mg was also confirmed by the absence of bacteria labeled by anti-*M. hominis* antibodies (Fig. 5B).

The presence of *M. hominis* in TvSS-62iso+Mh was confirmed by combining DAPI (Fig. 5C) and staining using anti-*M. hominis* antibodies (Fig. 5D) after 15 days of symbiosis, demonstrating the association of bacteria with trichomonad cells over the tested time frame. The low number of intracellular *M. hominis* bacteria was confirmed via the qPCR results (mean MOI of 0.8:1).

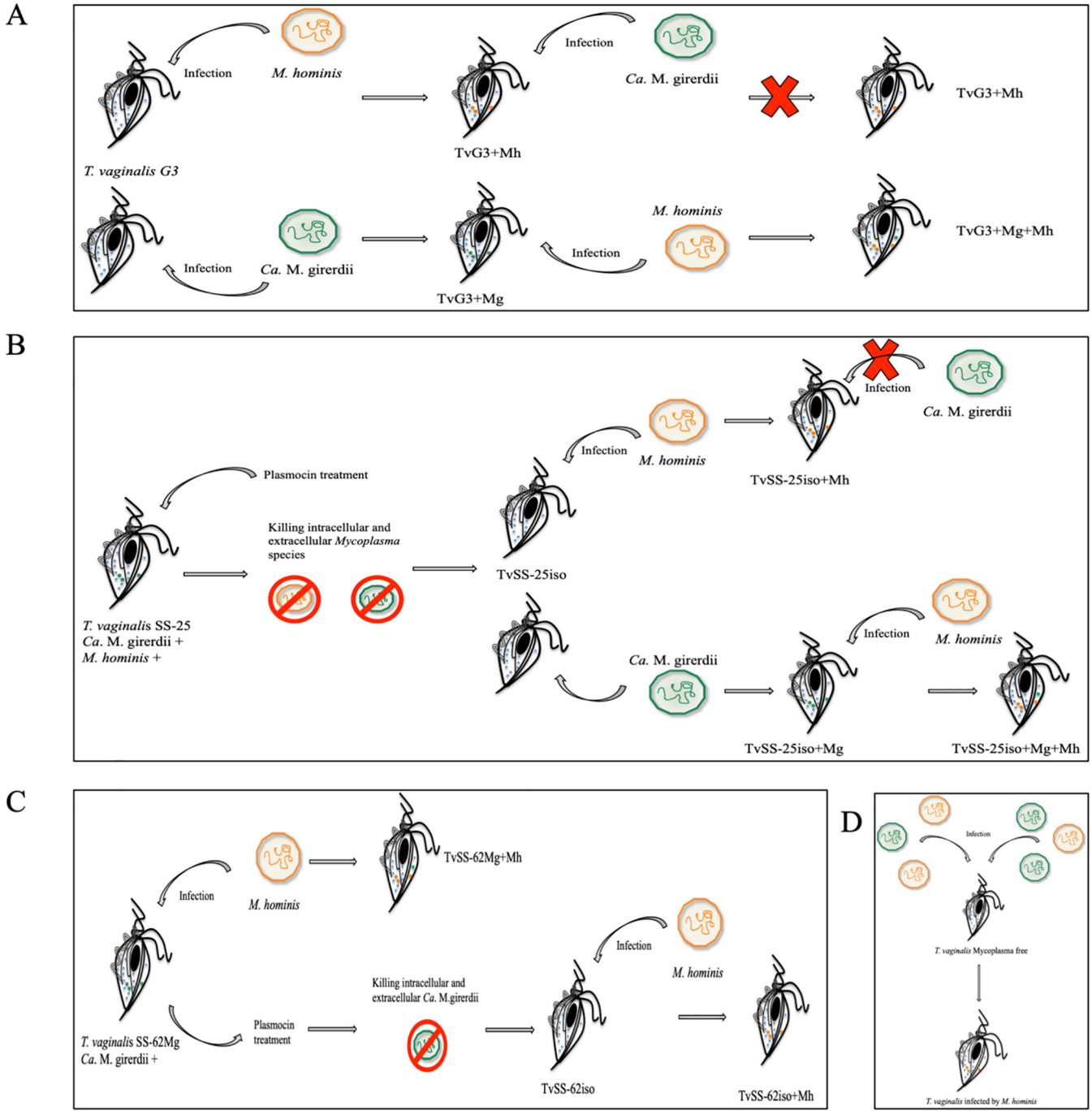

FIG 4 *In vitro* model system developed to study the ability of *Mycoplasma* to infect *T. vaginalis* cells. Three *T. vaginalis* isolates were used to evaluate the capability of infection of *Mycoplasma* species: *T. vaginalis* strain G3 (TvG3), mycoplasma free; *T. vaginalis* SS-25 (TvSS-25MgMh), naturally infected with "*Ca.* M. girerdii" and *M. hominis*; and *T. vaginalis* SS-62 (TvSS-62Mg), naturally "*Ca.* M. girerdii" infected. (A) Approach used to infect *T. vaginalis* strain G3 with *M. hominis* and "*Ca.* M. girerdii." (B and C) Experimental approaches used to clear mycoplasma species from *T. vaginalis* MgMh (B) and *T. vaginalis* SS-62Mg (C) to obtain mycoplasma-free cultures (TvSS-25iso and TvSS-62iso) that were subsequently infected with *M. hominis* (TvSS-25iso+Mh and TvSS-62iso+Mh) and "*Ca.* M. girerdii" (TvSS-25iso+Mg). (D) When *M. hominis* and "*Ca.* M. girerdii" were added at the same time to *Mycoplasma*-free *T. vaginalis* cultures, only *M. hominis* was able to establish a stable infection with *Trichomonas* cells.

The localization of both mycoplasma species in TvSS-62Mg+Mh experimentally exposed to *M. hominis* is illustrated in Fig. 5E and F. The presence of *M. hominis* was demonstrated by using specific antibodies. As previously demonstrated by the qPCR-based quantifications, the MOI of "*Ca.* M. girerdii" in parasites experimentally coinfected with *M. hominis* is significantly lower (Table 2) (TvG3+Mg+Mh, MOI of 0.13 to

TABLE 2 *T. vaginalis* strains used as recipients to produce isogenic trichomonad strains with single and double infections

Recipient strain[a]	No. of bacteria used to infect *T. vaginalis*[b]	Isogenic strain obtained[c]	95% CI of no. of bacteria/trichomonad cell (mean)[d]
TvG3	2.07E+06 of "*Ca*. M. girerdii"	TvG3+Mg	"*Ca*. M. girerdii," 2.66–5.08 (3.9)
TvG3	1.09E+05 of *M. hominis*	TvG3+Mh	*M. hominis*, 0.03–0.45 (0.24)
TvG3+Mg	3.88E+04 of *M. hominis*	TvG3+Mg+Mh	"*Ca*. M. girerdii," 0.13–0.27 (0.2) *M. hominis*, 0.004–0.01 (0.007)
TvSS-25iso	2.16E+06 of "*Ca*. M. girerdii"	TvSS-25iso+Mg	"*Ca*. M. girerdii," 0.24–0.42 (0.33)
TvSS-25iso	5.25E+03 of *M. hominis*	TvSS-25iso+Mh	*M. hominis*, 1.31–1.34 (1.33)
TvSS-25iso+Mg	3.60E+05 of *M. hominis*	TvSS-25iso+Mg+Mh	"*Ca*. M. girerdii," 0.005 *M. hominis*, 1.1–1.53 (1.3)
TvSS-62iso	1.50E+06 of *M. hominis*	TvSS-62iso+Mh	*M. hominis*, 0.82–1.1 (0.95)
TvSS-62Mg	3.60E+05 of *M. hominis*	TvSS-62Mg+Mh	"*Ca*. M. girerdii," 0.17–0.42 (0.3) *M. hominis*, 0.08–0.14 (0.11)

[a]*T. vaginalis* G3 is naturally mycoplasma free, *T. vaginalis* SS-25iso (TvSS-25iso) and *T. vaginalis* SS-62iso (TvSS-62iso) are strains experimentally cleaned from *Mycoplasma* species, and *T. vaginalis* SS-62 (TvSS-62Mg) is naturally "*Ca*. M. girerdii" infected (mean MOI, 11.83).
[b]Number of bacteria used to infect the recipient strains evaluated by qPCR.
[c]Isogenic strains experimentally obtained after infection with the indicated *Mycoplasma* species.
[d]Ranges and means (in parentheses) of MOI values for each *T. vaginalis* strain experimentally infected after 15 days of culture (continuous passage every day) are shown. The number of strains tested to evaluate the MOI of bacteria was 3 under each condition.

0.27 [mean, 0.2]; TvSS-25iso+Mg+Mh, mean MOI of 0.0005; TvSS-62Mg+Mh, MOI of 0.17 to 0.42 [mean, 0.3]) than that observed in *T. vaginalis* naturally infected with "*Ca.* M. girerdii" prior to coinfection (Table 1) (MOI, 3.7 to 18.24 [mean MOI of 11]) (Fig. 5A).

Effects of mycoplasma species on the growth rate of *T. vaginalis* cultures. We compared the growth of TvSS-62Mg, naturally infected with "*Ca.* M. girerdii," with that of the isogenic mycoplasma-free *T. vaginalis* strain (TvSS-62iso). In the same experiment, we also evaluated the growth rates of *M. hominis*-infected *T. vaginalis* (TvSS-62iso+Mh) and dually *M. hominis*- and "*Ca.* M. girerdii"-infected *T. vaginalis* (TvSS-62Mg+Mh). The parasites, in various associations with bacteria, were cultured for a total of 36 h, and total DNA was extracted from the parasites to quantify "*Ca.* M. girerdii" and *M. hominis* DNAs by qPCR. The variation between the growth curves of the mycoplasma-free *T. vaginalis* isogenic strain (TvSS-62iso) and the *T. vaginalis* doubly infected strain (TvSS-62Mg+Mh) was significant (*P* value of <0.01), with a higher rate of replication for TvSS-62Mg+Mh than for TvSS-62iso. There was also significant variation (*P* value of <0.05) between the growth curves of the mycoplasma-free *T. vaginalis* strain (TvSS-62iso) and both *T. vaginalis* infected by "*Ca*. M. girerdii" alone (TvSS-62Mg) and *T. vaginalis* infected by *M. hominis* alone (TvSS-62iso+Mh), with higher replication rates for TvSS-62Mg and TvSS-62iso+Mh than for TvSS-62iso. In contrast, the differences between TvSS-62Mg and both TvSS-62iso+Mh and TvSS-62Mg+Mh were not statistically significant (Fig. 6).

These results indicate that both "*Ca*. M. girerdii" and *M. hominis*, in single or double infections, are associated with an increased rate of replication of *T. vaginalis* in Diamond's Trypticase-yeast extract-maltose (TYM) medium.

RNA sequencing (RNA-Seq) analysis of *T. vaginalis* associated with *Mycoplasma*. Reads from TvSS-62Mg, TvSS-62iso+Mh, TvSS-62Mg+Mh, and TvSS-62iso (axenically cleaned from "*Ca*. M. girerdii" and used as a control) were classified by Kraken2 (Fig. 7). *T. vaginalis* reads were the most abundant in all libraries, ranging from 53 to 73% of the total reads, as expected. Consistent with the relatively lower MOI for *M. hominis* TvSS-62iso+Mh (MOI range, 0.82 to 1.1 [mean, 0.95]; $n = 3$), the reads mapping onto the reference genome of *M. hominis* had relatively lower abundances in the TvSS-62iso+Mh sample (0.11% of the total reads), whereas "*Ca.* M. girerdii" reads were more abundant in TvSS-62Mg (0.57%), suggesting a lower overall biomass of *M. hominis* (Fig. 7B). *M. hominis* reads decreased by a factor of nearly 100 in TvSS-62Mg+Mh (0.0016%) compared with TvSS-62iso+Mh symbiosis, whereas "*Ca.* M. girerdii" reads were more frequent in TvSS-62Mg (4.7% of the total reads). Evidence from read classification indicated the presence of several distinct *Trichomonas vaginalis* viruses (TVVs) and associated satellite viruses. Viral reads were relatively abundant, ranging from 7.7

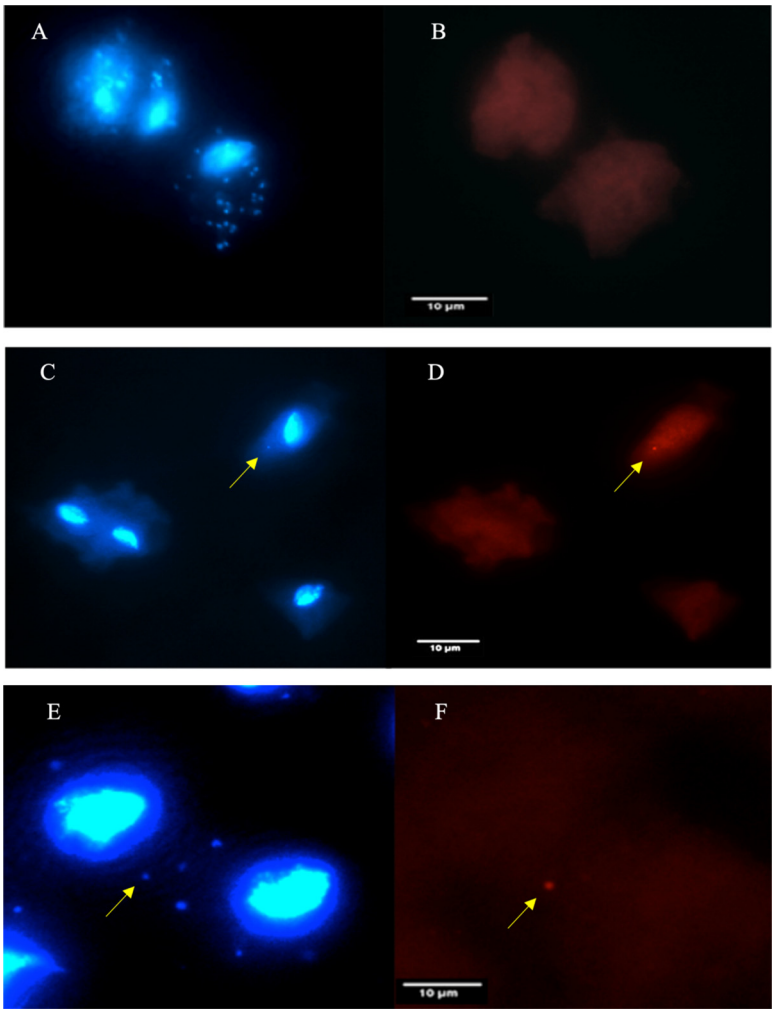

FIG 5 Detection of *Mycoplasma* species in *T. vaginalis* cells. (A) Cellular localizations of "*Ca*. M. girerdii" in TvSS-62Mg and a high number of bacteria stained with DAPI (22 stained cells). (B) The absence of *M. hominis* infection was demonstrated by using anti-*M. hominis* antibodies. (C and D) The presence of a very low number of *M. hominis* bacteria in *T. vaginalis* experimentally infected with the bacterium (TvSS-62iso+Mh), with just one stained cell in this one *T. vaginalis* cell. Yellow arrows indicate the localization of *M. hominis* in a trichomonad cell stained with DAPI (C) and with anti-*M. hominis* antibody (D). (E and F) Localization of "*Ca*. M. girerdii" and *M. hominis* stained with DAPI (E) and with anti-*M. hominis* antibody (F) in *T. vaginalis* SS-62Mg+Mh cells. Yellow arrows indicate the localization of *M. hominis* in a trichomonad cell stained with DAPI (C and E) and with anti-*M. hominis* antibody (D and F), with the other DAPI-labeled cells representing "*Ca*. M. girerdii" cells.

to 11% of the total reads. Intriguingly, the presence of *Mycoplasma* appeared to have an influence on the relative abundance of some viral transcripts. Compared with the other conditions, TVV4 reads were greatly decreased in *T. vaginalis* associated with *M. hominis* only (TvSS-62iso+Mh). TVV satellite S1 reads were more abundant in the TvSS-62Mg strain, and TVV satellite S1′ appeared to be enhanced by the presence of *M. hominis* alone.

Assessment of the quantification data mapped onto the *T. vaginalis* G3 reference genome suggested that the data are of high quality and suitable for assessing differential expression. Principal-coordinate analysis (PCA) demonstrated that the variation between conditions was much greater than that between replicates. PCA also suggested greater similarity within the *Mycoplasma*-infected samples than with *Mycoplasma*-free *T. vaginalis* (TvSS-62iso) and greater similarity between TvSS-62Mg and TvSS-62Mg+Mh conditions than for the TvSS-62iso+Mh condition (Fig. 8A). The biological coefficient of variation (BCV) among the data was low (common estimate across all genes, 0.015) (Fig. 8B), and the

A

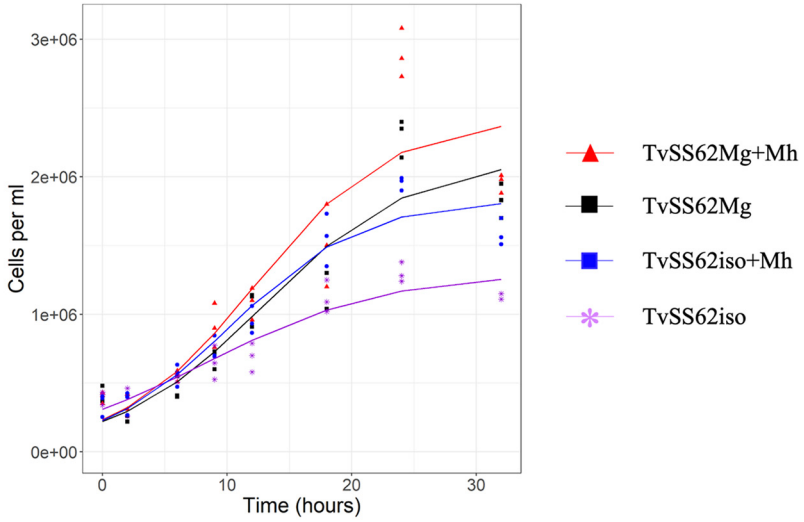

B

Growth curves comparisons	P-value
TvSS-62iso (myco-free) vs TvSS-62Mg+Mh	0.0039**
TvSS-62iso (myco-free) vs TvSS-62Mg	0.0382*
TvSS-62iso (myco-free) vs TvSS-62iso+Mh	0.0509*
TvSS-62Mg vs TvSS-62Mg+Mh	0.1060
TvSS-62iso+Mh vs TvSS-62Mg	0.830

FIG 6 Influence of *Mycoplasma* species on *T. vaginalis* growth curves. Under all conditions, 400,000 parasite cells/mL were used as the starting point for the growth experiments, and data were collected at the indicated times. The growth curves are characterized by 3 parameters (K, N_0, and r, respectively [see the equation as a function of the growth rate in Materials and Methods]) for each of the following strains: TvSS-62iso (1,301,849, 309,953, and 0.139), TvSS-62iso+Mh (1,834,817, 228,428, and 0.189), TvSS-62Mg (2,137,960, 220,307, and 0.167), and TvSS-62Mg+Mh (2,430,753, 232,721, and 0.183). The rates of replication of isogenic mycoplasma-free (myco-free) *T. vaginalis* TvSS-62iso (purple), *M. hominis*-infected *T. vaginalis* TvSS-62iso+Mh (blue), naturally "*Ca.* M. girerdii"-infected *T. vaginalis* TvSS-62Mg (black), and *M. hominis*- and "*Ca.* M. girerdii"-infected *T. vaginalis* TvSS-62Mg+Mh (red) were compared (A), and the presence of a single *Mycoplasma* species or both bacteria in trichomonad cells was associated with increased growth rates of the parasites, compared with the replication rate of mycoplasma-free *T. vaginalis* (*, $P < 0.05$; **, $P < 0.01$) (B).

majority of genes showed low variation of expression between samples after statistical normalization (Fig. 8C), indicating that normalization was successful. A total of 5,938 genes were significantly differentially expressed across all *Mycoplasma* conditions compared with the control TvSS-62iso (Table S3). *M. hominis* alone induced the largest response, with 3,814 significantly modulated genes, followed by 3,617 in response to *M. girerdii* and, intriguingly, only 2,558 in response to simultaneous *M. hominis* and *M. girerdii* infection (Fig. 8D to F; Table S3).

***T. vaginalis* genes regulated in the presence of *Mycoplasma*.** The set of genes regulated in *T. vaginalis* in response to the presence of *Mycoplasma* largely overlapped between the TvSS-62iso+Mh, TvSS-62Mg, and TvSS-62Mg+Mh conditions compared with the control TvSS-62iso, corresponding to a core transcriptional response to the presence of either *Mycoplasma* species (Fig. 9A). Interestingly, this core set of genes appeared to be biased toward upregulation (Fig. 9). There were also large sets of genes that were uniquely regulated in response to individual conditions, indicating distinct transcriptional responses to *M. hominis*, "*Ca.* M. girerdii," and the simultaneous presence of both mycoplasmas.

In order to examine the transcriptional response that was specific to the synergy of

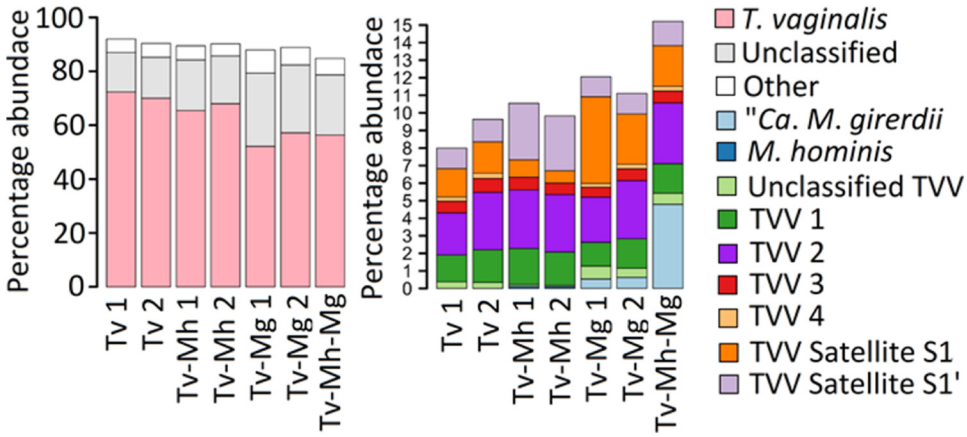

FIG 7 Number of reads allocated by Kraken2 to each organism under the different culture conditions. The most abundant groups (A) and less abundant groups (B) are shown separately as a percentage of the library size (TVV, *Trichomonas vaginalis* virus). "Unclassified" reads could not be aligned by Kraken2 to any sequence in the NCBI nonredundant nucleotide database.

both mycoplasmas, differential expression was tested in the TvSS-62Mg+Mh condition versus the respective single-*Mycoplasma* conditions (Fig. 9B). Very few genes were differentially regulated in TvSS-62Mg+Mh compared with TvSS-62Mg alone, whereas there was a major transcriptional response resulting from the introduction of "*Ca*. M. girerdii" to the TvSS-62iso+Mh condition, consistent with a dominant effect of the presence of "*Ca*. M. girerdii." Only 11 genes overlapped between these comparisons, which represent a gene set specific to the synergistic effect of both mycoplasmas compared with only a single species.

Functional prediction of *T. vaginalis* differential gene expression. Gene ontology (GO) enrichment analysis was used to summarize the functions of genes that were differentially expressed in response to the presence of *Mycoplasma* (Table 3). The core set of genes homodirectionally regulated in response to all three *Mycoplasma* conditions (Fig. 9A, region 5) was associated with a variety of metabolic responses. The catabolism of various amino acids, including threonine, aspartate, and glutamine family amino acids, increased in the presence of *Mycoplasma*. There was also an apparent increase in central energy metabolism via the hydrogenosome, indicated by processes such as "electron transport chain" and the misidentified "tricarboxylic acid cycle" (TCA cycle) (e.g., TVAG_165030 [malate dehydrogenase family protein]). We examined the expression of enzymes annotated as part of the TCA cycle, and the related malate metabolic process, in detail (Fig. 10A). Consistent with the enrichment analysis results, the majority (8 out of 11) of the genes were significantly upregulated in the presence of *Mycoplasma*. All the upregulated genes could be aligned well at the protein level with one another and *T. vaginalis* malate dehydrogenase (GenBank accession number AAC46986.1 [strain NIH-C1]) (99% identical to TVAG_253650 [strain G3]) investigated by previously by Wu and colleagues (49). All upregulated genes possessed the Arg91Leu mutation, which confers specificity to lactate. Among all TCA/malate metabolic process enzymes, this group also included the most highly expressed gene (TVAG_381310 [mean transcripts per million {TPM}, 2,600]) and the most highly upregulated gene under all *Mycoplasma* conditions versus the control (TVAG_165030 [$\log_2$ fold changes of 3.4, 2.6, and 3.0 under the TvSS-62iso+Mh, TvSS-62Mg, and TvSS-62Mg+Mh conditions, respectively]). The three downregulated genes aligned well with the *Escherichia coli* decarboxylating malic enzyme (RefSeq accession number NP_415996.2) (50), and two were predicted to be localized to the hydrogenosome by Burstein and colleagues (51). The single gene not predicted to be localized in hydrogenosomes (TVAG_068130) was truncated by approximately 296 amino acid residues at the N terminus compared with the other two and the *E. coli* enzyme, suggesting that it is a gene fragment. Overall, these results suggest that the presence of *Mycoplasma* may induce

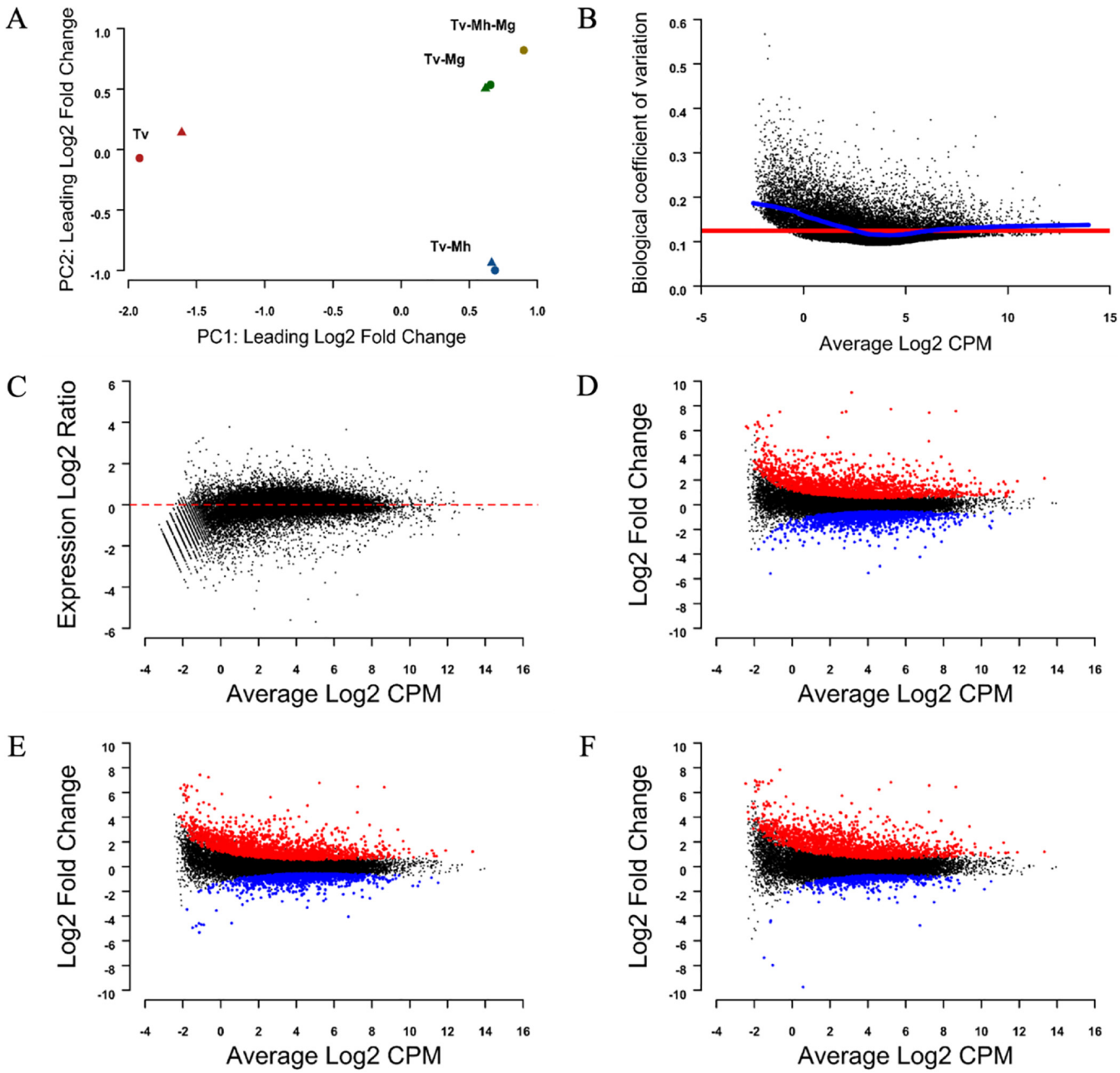

FIG 8 Quality assessment for RNA-Seq expression quantification data. (A) Principal-coordinate analysis (PCoA) showing root mean square deviations of $\log_2$ fold changes for all genes between samples. Samples 1 and 2 under each condition are indicated by circles and triangles, respectively. (B) Biological coefficient of variation (BCV) versus $\log_2$ counts (counts per million [CPM]) for each gene throughout all samples. The trended and common BCV estimates are shown in blue and red, respectively. (C) Smear plot showing $\log_2$ expression ratios for a single *T. vaginalis* (TvSS-62iso) sample compared with the average for all others versus $\log_2$ read counts. The dashed line indicates zero. (D to F) Smear plots showing $\log_2$ fold changes compared with the control (*T. vaginalis* [Tv]) for TvSS-62iso+Mh (Tv-Mh) (D), TvSS-62Mg (Tv-Mg) (E), and TvSS-62Mg+Mh (Tv-Mh-Mg) (F) versus average expression, with significantly upregulated and downregulated genes (FDR < 0.05) highlighted in red and blue, respectively.

an increase in cytosolic lactate fermentation and a decrease in hydrogenosomal metabolism proceeding via malate catabolism. Finally, we also observed that there was an increase in "response to oxidative stress" with the two related entries "cellular oxidant detoxification" and "response to oxidative stress" (Table 3).

The results from KEGG enrichment analysis were largely in agreement with those from the GO term enrichment analysis and also highlighted upregulated enzymes potentially involved in the synthesis (such as TVAG_388260 [UDP-glucose pyrophosphorylase]) and utilization (such as TVAG_185930 [alpha amylase] and TVAG_222040

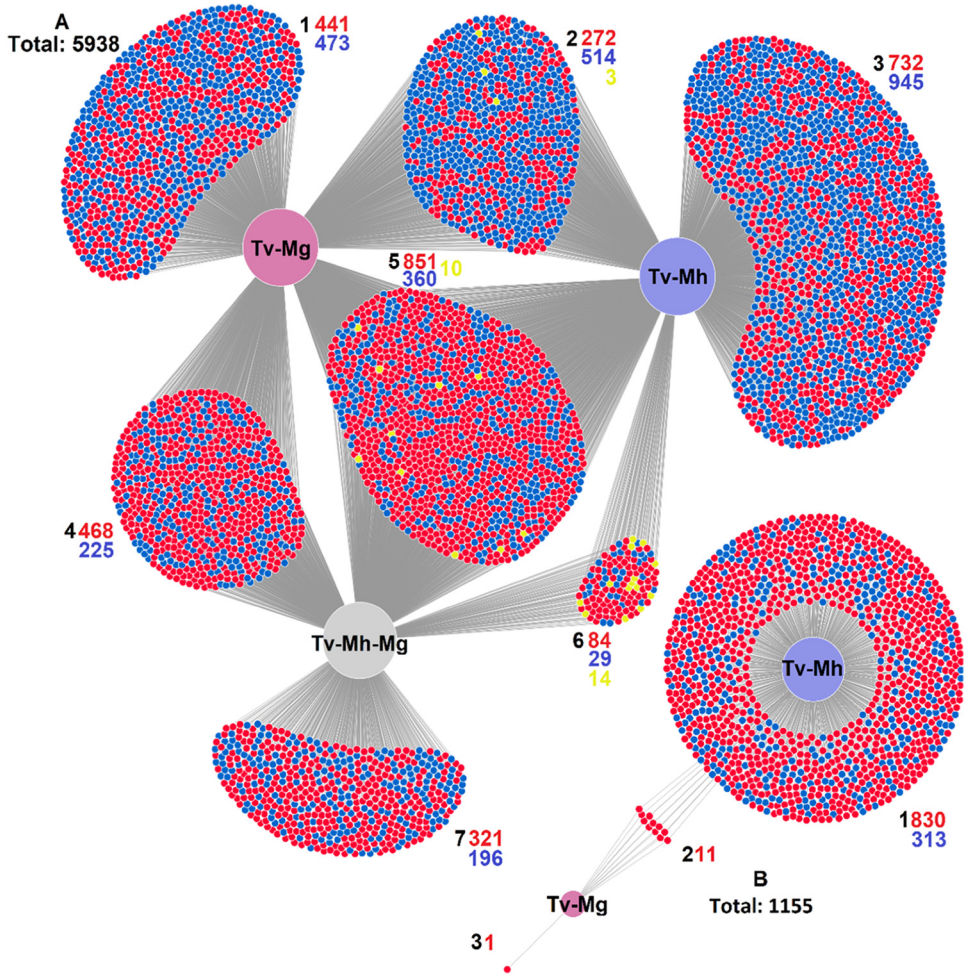

FIG 9 DiVenn diagrams depicting the extent of overlap of differentially expressed genes in pairwise comparisons between the different *T. vaginalis-Mycoplasma* symbioses. Large nodes symbolize specific *T. vaginalis-Mycoplasma* symbioses, and small nodes indicate individual genes. Edges link genes with comparisons under which they are significantly differentially expressed (FDR $<$ 0.05) compared to the control TvSS-62iso. Small nodes are shown in red and blue to indicate upregulated and downregulated genes, respectively. Yellow nodes indicate disparity in the direction of regulation between multiple comparisons. Comparison nodes are in light blue for TvSS-62iso+Mh (Tv-Mh), mauve for TvSS-62Mg (Tv-Mg), and gray for TvSS-62Mg+Mh (Tv-Mh-Mg). Specific clouds/groupings of genes are labeled 1 to 6 in panel A and 1 to 3 in panel B. Separate DiVenn diagrams are shown for comparisons between either the control TvSS-62iso (Tv) and the different symbioses (A) or the TvSS-62Mg+Mh condition versus the two single symbioses using single-*Mycoplasma* conditions as the control (B). Numbers are used to label regions of gene nodes in black, and total gene counts for each region are shown in colors corresponding to the gene nodes. Total values indicate all genes in each DiVenn diagram.

[4-alpha-glucanotransferase]) of cellular glycogen stores, under the category "starch and sucrose metabolism" (Table S4). Intriguingly, processes downregulated in response to *Mycoplasma* included pathways involved in the biosynthesis and catabolism of lipids and motility (Table 3). To investigate any significance of changes in lipid metabolism among the three species, we examined differences in KEGG-annotated lipid metabolic enzymes. "*Ca*. M. girerdii" possesses several enzymatic functions involved in glycerophospholipid biosynthesis apparently absent in *T. vaginalis*, including acyl phosphate:glycerol-3-phosphate acyltransferase, cardiolipin synthase, and phosphate acyltransferase. *M. hominis* possesses only one annotated lipid metabolism-associated enzyme absent in *T. vaginalis*, phosphate acyltransferase.

The enrichment analysis results also indicated that the regulatory responses to *Mycoplasma* involve transcription-level control and protein phosphorylation and dephosphorylation (Table 3).

TABLE 3 The most significantly enriched GO biological process terms among genes regulated in response to all *Mycoplasma* symbioses[a]

Description	No. of expressed genes[b]	No. of DE genes[c]	*P* value	Direction of regulation
Glycerolipid biosynthetic process	30	9	2.28E−06	Negative
Lipid biosynthetic process	72	12	2.52E−06	
Phospholipid biosynthetic process	45	9	2.70E−05	
Phosphatidylcholine biosynthetic process	4	4	0.00051	
Microtubule-based movement	149	12	0.000651	
Cellular lipid catabolic process	15	5	0.00117	
S-Adenosylmethionine biosynthetic process	6	3	0.0212	
Glycerol biosynthetic process from pyruvate	8	3	0.026	
Short-chain fatty acid catabolic process	8	3	0.0266	
Response to lipid	8	3	0.0272	
Steroid metabolic process	8	3	0.0291	
Alditol biosynthetic process	8	3	0.0314	
Triglyceride biosynthetic process	8	3	0.0322	
Fatty acid catabolic process	10	3	0.0346	
Cellular response to glucose stimulus	8	3	0.036	
Propionate catabolic process	8	3	0.0371	
Cellular glucose homeostasis	8	3	0.0382	
Iron-sulfur cluster assembly	27	12	5.53E−07	Positive
Protein phosphorylation	1,056	74	3.00E−06	
Cofactor metabolic process	97	16	6.61E−05	
Cellular oxidant detoxification	26	9	9.20E−05	
Cellular response to toxic substance	26	9	9.42E−05	
Aerobic respiration	28	9	0.000143	
Oxaloacetate metabolic process	21	8	0.000179	
Glutamine family amino acid metabolic process	24	8	0.000352	
Drug metabolic process	77	13	0.000382	
Tricarboxylic acid cycle	26	8	0.000543	
Malate metabolic process	26	8	0.000553	
Protein dephosphorylation	301	27	0.000638	
NADH metabolic process	30	8	0.00122	
Aspartate family amino acid catabolic process	9	5	0.00252	
Response to oxidative stress	35	8	0.00289	
Negative regulation of transcription, DNA templated	61	10	0.00417	
Electron transport chain	50	9	0.00476	
Negative regulation of transcription from RNA polymerase II promoter	30	7	0.00641	
Negative regulation of RNA biosynthetic process	70	10	0.00986	
Threonine catabolic process	8	4	0.0146	

[a]The top 20 lowest *P* value terms are shown for upregulated and downregulated genes, ranked by increasing *P* values.
[b]Total number of genes associated with the GO term with detected expression in this experiment.
[c]Number of differentially expressed (DE) genes associated with the GO term.

Notably, the TvSS-62Mg and double-symbiosis conditions showed highly similar transcriptional profiles (Fig. 9B, region 2). In addition, the set of 11 genes specific to this condition versus the individual symbioses encoded reactive oxygen species (ROS) detoxification enzymes and hydrogenosomal energy generation enzymes (Fig. 10B).

Impact of symbiosis on ADH pathway gene expression. We investigated the impact of *Mycoplasma* symbiosis on arginine dihydrolase (ADH) pathway enzyme expression due to its shared importance as a means of energy generation in *T. vaginalis* and *M. hominis* (22) (Fig. 11). The majority of *T. vaginalis* ADH enzymes were not significantly regulated. However, intriguingly, for ornithine carbamoyl transferase (OCT) (the most highly expressed enzyme of the pathway), the two homologs showed opposite mild but significant regulatory profiles in response to *Mycoplasma*. TVAG_041310 was upregulated with $\log_2$ fold changes of 0.8, 1.0, and 1.1 under the TvSS-62iso+Mh (Tv-Mh), TvSS-62Mg (Tv-Mg), and TvSS-62Mg+Mh (Tv-Mh-Mg) conditions versus the control, whereas TVAG_368740 was downregulated with corresponding $\log_2$ fold change values of −1.3, −1.4, and −0.9, respectively. Based on the reconstructed open reading frame (ORF) from the RNA-Seq data, the two enzymes were 97% identical at the protein level, with 8 mismatching residues. However, none of the mutations coincided

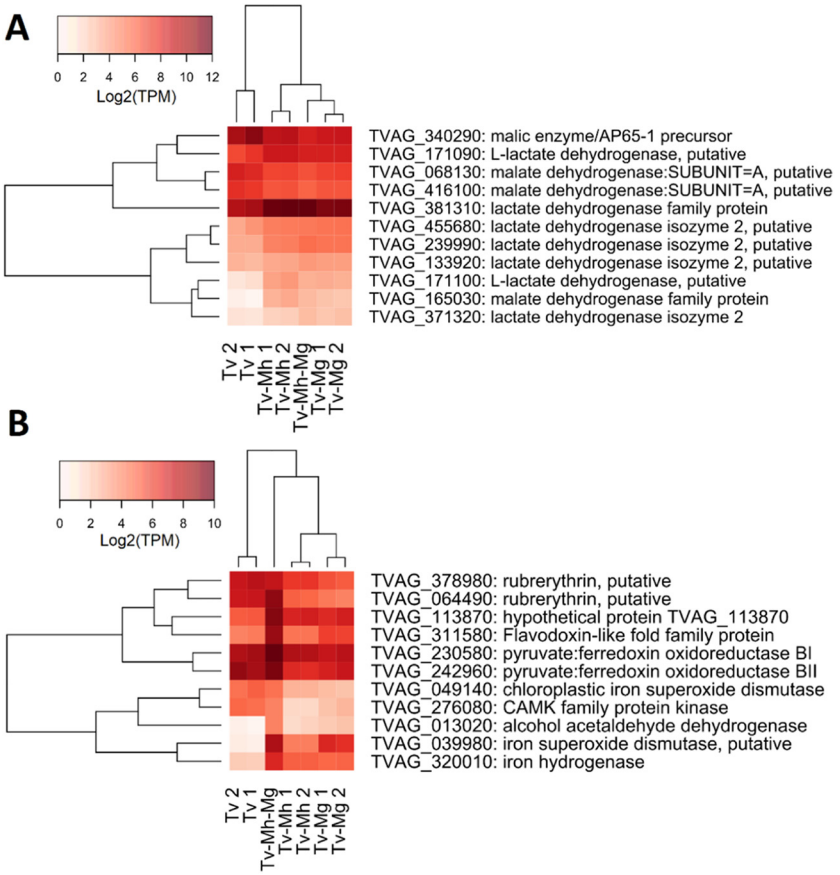

FIG 10 Heatmap of all genes significantly differentially expressed under both the TvSS-62iso+Mh and TvSS-62Mg conditions versus the TvSS-62Mg+Mh condition. Heatmaps show all significantly differentially expressed genes annotated with TCA cycle or malate metabolic process GO terms (A) and all genes significantly differentially expressed under both the TvSS-62iso+Mh (Tv-Mh) and TvSS-62Mg (Tv-Mg) conditions versus the TvSS-62Mg+Mh (Tv-Mh-Mg) condition (B). Expression is shown in units of $\log_2$ transcripts per million (TPM). CAMK, Ca2+/calmodulin-dependent protein kinase

with highly conserved or putative functionally important residues in published data on OCT enzymes (52). The two enzymes were 92% identical at the nucleotide level, with mutations present within all 50-bp windows, and thus were likely easily distinguished during the alignment of the 150-bp RNA-Seq reads. Interestingly, the sum of the TPM values for the two enzymes dropped slightly from a mean of 219 to 181 under the Tv-Mh condition versus the control, possibly corresponding to a decrease in enzyme activity. In contrast, the corresponding values were 201 and 217 under the Tv-Mg and Tv-Mh-Mg conditions, respectively. Two putatively annotated arginase enzymes, which are not considered part of the ADH pathway, were also significantly upregulated by a similar magnitude under all *Mycoplasma* conditions. The strongest regulation was for the putative arginase TVAG_025140, with $\log_2$ fold changes of 2.8, 3.6, and 4.4 under the Tv-Mh, Tv-Mg, and Tv-Mh-Mg conditions versus the control, respectively.

Analysis of genes potentially implicated in *T. vaginalis* pathobiology. To investigate the regulation of genes potentially implicated in *T. vaginalis* pathobiology, we examined the expression of annotated surface proteins, including TvBspA-like proteins that can mediate cell-cell interactions (37, 53), and experimentally verified exosomal proteins, implicated in adhesion to host cells and immunomodulation (54–56) (Fig. 12). Out of a total of 911 TvBspA-like proteins, 255 were significantly differentially regulated under at least one of the tested *Mycoplasma* symbioses, and similarly, 103 out of 314 experimentally verified surface proteins (EVSPs) and 52 out of 215 exosome proteins were also significantly modulated. Notably, TvBspA-like genes, surface proteins, and

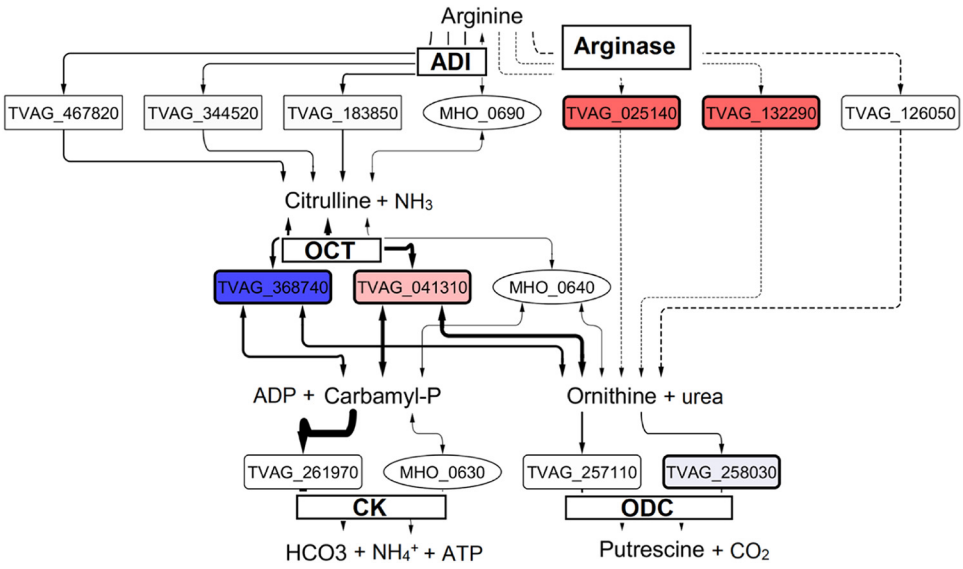

FIG 11 Expression of arginine dihydrolase (ADH) pathway genes. *T. vaginalis* hydrogenosomal and cytoplasmic enzymes and *M. hominis* enzymes are enclosed in squared rectangles, rounded rectangles, and ovals, respectively. *T. vaginalis* enzymes that are significantly differentially expressed under the Tv-Mh versus Tv conditions are bordered in bold, and the fill color is scaled from blue (downregulated) to red (upregulated) according to their $\log_2$ fold changes in this comparison. For *T. vaginalis* enzymes, the arrow thickness is scaled to their expression level in TPM. Dashed lines for arginase indicate uncertainty as to whether activity for this enzyme is present in *T. vaginalis* (68, 69). ADI (Arginine deiminase); CK (Carbamate kinase); OCT (Ornithine carbamyltransferase); ODC (ornithine decarboxylase)

exosome proteins were significantly modulated as gene sets under each *Mycoplasma* condition versus the control (false discovery rate [FDR] $<$ 0.001). However, gene set modulation in a particular direction, either upregulation or downregulation, was not significant (FDR $>$ 0.05), indicating no clear global directional response (Table 4). Many EVSPs, including some TvBspA-like proteins, showed expression profiles that were specific to each *Mycoplasma* species (Fig. 13 and 14). An overall positive regulation of exosome proteins under the TvSS-62Mg+Mh condition versus the control was near the threshold for significance (*P* value of 0.075).

Of particular interest, 9 out of 11 genes significantly upregulated among more adherent *T. vaginalis* strains (54) were significantly regulated in response to *Mycoplasma*, 8 of which were upregulated under one or more of the *Mycoplasma* conditions compared with the control (Fig. 13 and 14; Table S5). These included two members of the polymorphic outer membrane (Pmp) protein family (57). One Pmp entry (TVAG_140850) was shown experimentally to boost the binding of parasites to vaginal epithelial cells when overexpressed (53). These are members of a larger family of hypothetical proteins in *T. vaginalis* (155 members [see reference 57]) related to the bacterial Bap (for biofilm-associated protein) surface proteins from various bacterial species and the InlB protein, a member of the internalin protein family in *Listeria*, which can mediate bacterial biofilm formation and binding to and internalization in eukaryotic host cells (58, 59). At least five additional members of this Bap-like protein family were also significantly upregulated in the presence of either of the *Mycoplasma* species (TVAG_359980, TVAG_238790, TVAG_238780, TVAG_238800, and TVAG_200680) (Table S3). We also investigated the modulation of the transcripts encoding the saposin-like protein family members (SAPLIPs), which potentially mediate the pore-forming activity underlying hemolysis (46, 57). Of the 11 transcribed SAPLIP genes, 7 transcripts were significantly upregulated (Fig. 15).

Expression of "*Ca.* M. girerdii" and *M. hominis* genes. Despite the low sequence coverage for *Mycoplasma* transcripts (Fig. 6), expression was detected for 495 out of 652 *M. hominis* genes (76%) and 553 out of 563 "*Ca*. M. girerdii" genes (98%) across all *Mycoplasma*-containing samples (Table S6). The ADH pathway was highly active in *M. hominis*, with the 3 contributing enzymes, arginine deiminase, ornithine carbamoyl transferase, and carbamate kinase, all included among the 25 ORFs with the highest

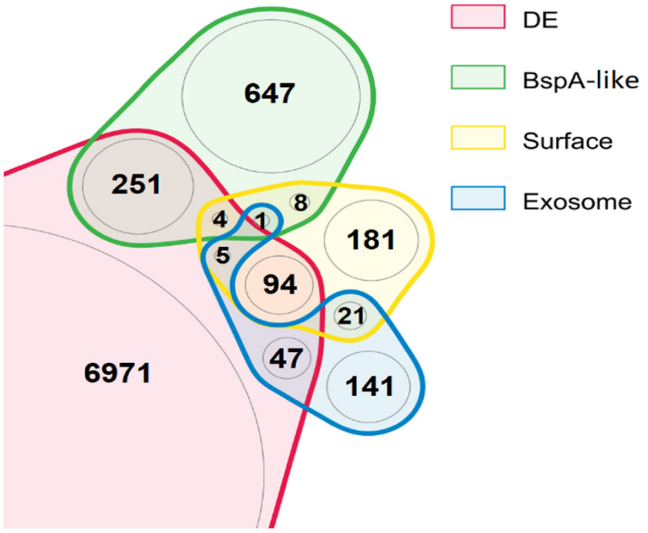

FIG 12 Differential expression of pathobiology-associated genes during *T. vaginalis-Mycoplasma* coculture. The Venn diagram shows the overlap in gene sets differentially expressed (DE) under any *Mycoplasma* condition, annotated as BspA (37), experimentally verified surface proteins (54), and experimentally verified exosome proteins (55). Only the region showing the total list of differentially expressed genes is cropped.

TPM values (Table S5). In "*Ca*. M. girerdii," various putative amino acid transporters, enzymes involved in amino acid catabolism (alanine dehydrogenase [B1217_0546], serine dehydratase [B1217_0101], and cysteine desulfidase [B1217_0039]), and the full annotated glycolytic pathway had high numbers of mapped reads, suggesting energy generation via these pathways. Pyruvate formate-lyase (B1217_0461) and its potentially associated autonomous glycyl radical cofactor (B1217_0541) were among the most abundant transcripts, suggesting that anaerobically adapted glycolysis was active. Concurrent with numerous *T. vaginalis* BspA-like-encoding genes being transcribed, including a number of entries modulated by the presence of "*Ca*. M. girerdii" (Fig. 12), we detected "*Ca*. M. girerdii" expression for 24 out of a total of 26 (27) annotated BspA-like proteins. The BspA-like gene B1217_0328 was also among the most highly expressed genes (15th most transcribed gene) (Table S5). Notably, the "*Ca*. M. girerdii" gene B1217_0162, a putative 2′,3′-cyclic nucleotide 2′-phosphodiesterase (catalyzing KEGG reaction K01119), was also highly expressed (45th most transcribed gene), in parallel with the *T. vaginalis* adenylate and guanylate cyclase-encoding genes TVAG_365230 and TVAG_451920, which were among the most highly upregulated genes in the presence of "*Ca*. M. girerdii" and putatively generate the cyclic nucleotide substrate for the *Mycoplasma* phosphodiesterase enzyme. Sequence analysis of B1217_0162 predicted that it is a candidate surface protein anchored to the extracellular face of the plasma membrane via an N-terminal lipoprotein signal peptide.

Variability of "*Ca.* M. girerdii" MOIs in TvSS-62Mg under stress conditions. We observed that the presence of "*Ca.* M. girerdii" in symbiosis with *T. vaginalis* (strain

TABLE 4 Adjusted *P* values for gene set testing of genes implicated in *T. vaginalis* pathobiology[a]

	Adjusted *P* value					
	Nondirectional DE			Upregulated		
Gene set (reference)	Tv-Mh	Tv-Mg	Tv-Mh-Mg	Tv-Mh	Tv-Mg	Tv-Mh-Mg
Surface proteins (54)	4.48×10^{-4}	9.77×10^{-7}	5.35×10^{-4}	0.245	0.761	0.493
BspA-like proteins (37)	7.02×10^{-6}	9.21×10^{-6}	5.15×10^{-5}	0.612	0.761	0.526
Exosome proteins (55)	3.49×10^{-5}	6.21×10^{-4}	5.36×10^{-4}	0.245	0.111	0.0752

[a]Values are given for each of the *Mycoplasma* conditions versus the control *T. vaginalis* SS-62iso, which is *Mycoplasma* free. Tv-Mh, TvSS-62iso+Mh; Tv-Mg, TvSS-62Mg; Tv-Mh-Mg, TvSS-62Mg+Mh.

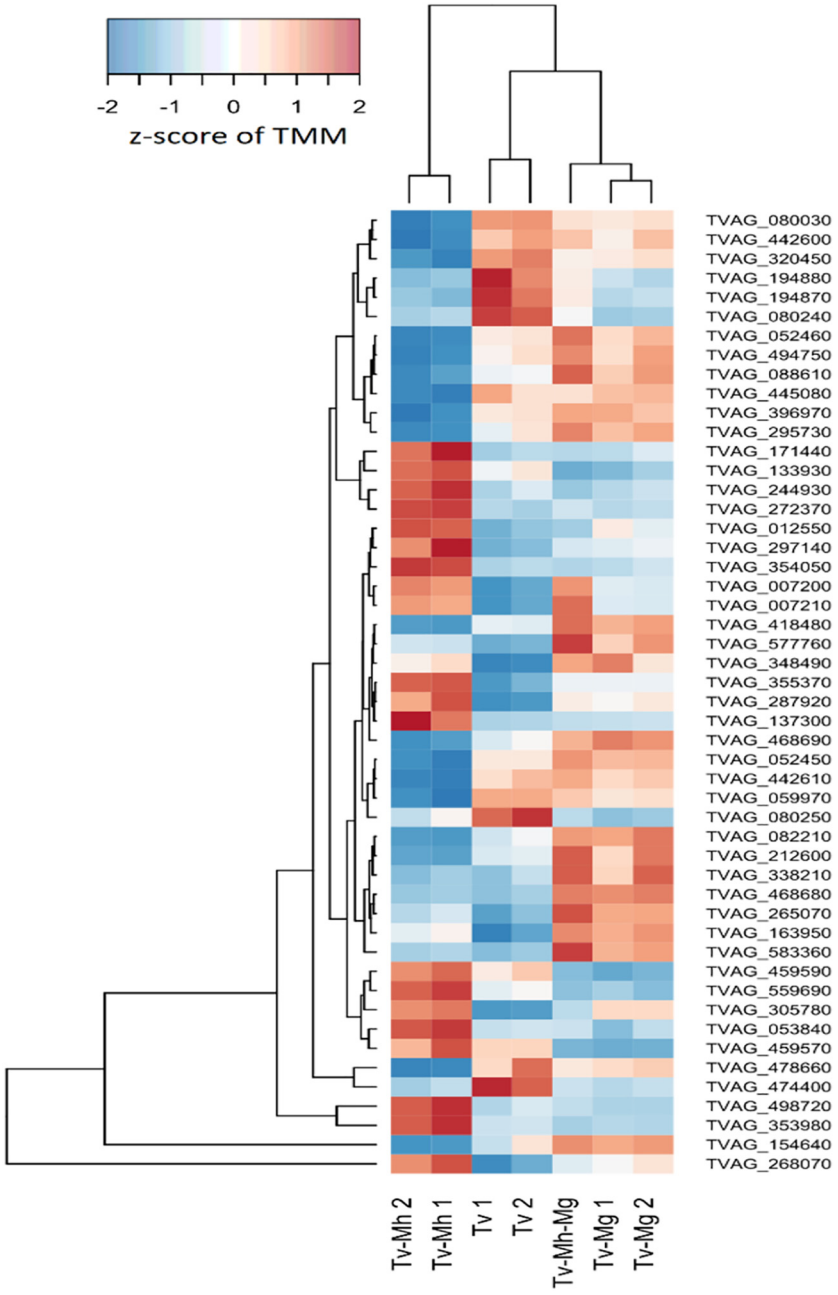

FIG 13 Differential expression of *T. vaginalis* annotated BspA genes during coculture with *Mycoplasma*. A heatmap of annotated *T. vaginalis* BspAs (37) with the top 50 lowest *P* values for differential expression under any *Mycoplasma* condition is shown. Expression units are z-scaled TMM.

TvSS-62Mg) did not influence the viability of the parasite during the extreme nutrient stress for the tested incubation times (phosphate-buffered saline [PBS] for 30 min and 60 min) (Fig. 16A). Notably, these starvation conditions strongly influence the "*Ca.* M. girerdii" mean MOI bacterium/trichomonad ratio, dramatically decreasing from 12:1 in standard Diamond's TYM medium down to 1:9 and 1:750 following 30-min and 60-min starvation conditions, respectively (Fig. 16B). These results indicate an increase of xenophagy of the bacteria by *T. vaginalis* in response to the tested stress conditions, a direct impact of the stress conditions on the bacteria, or a combination of these two options. A similar phenomenon was observed from limiting dilution experiments with TvSS-62Mg where the presence of "*Ca.* M. girerdii" was detected until a dilution of 12.5 *T. vaginalis* cells/well in 100 μL of medium.

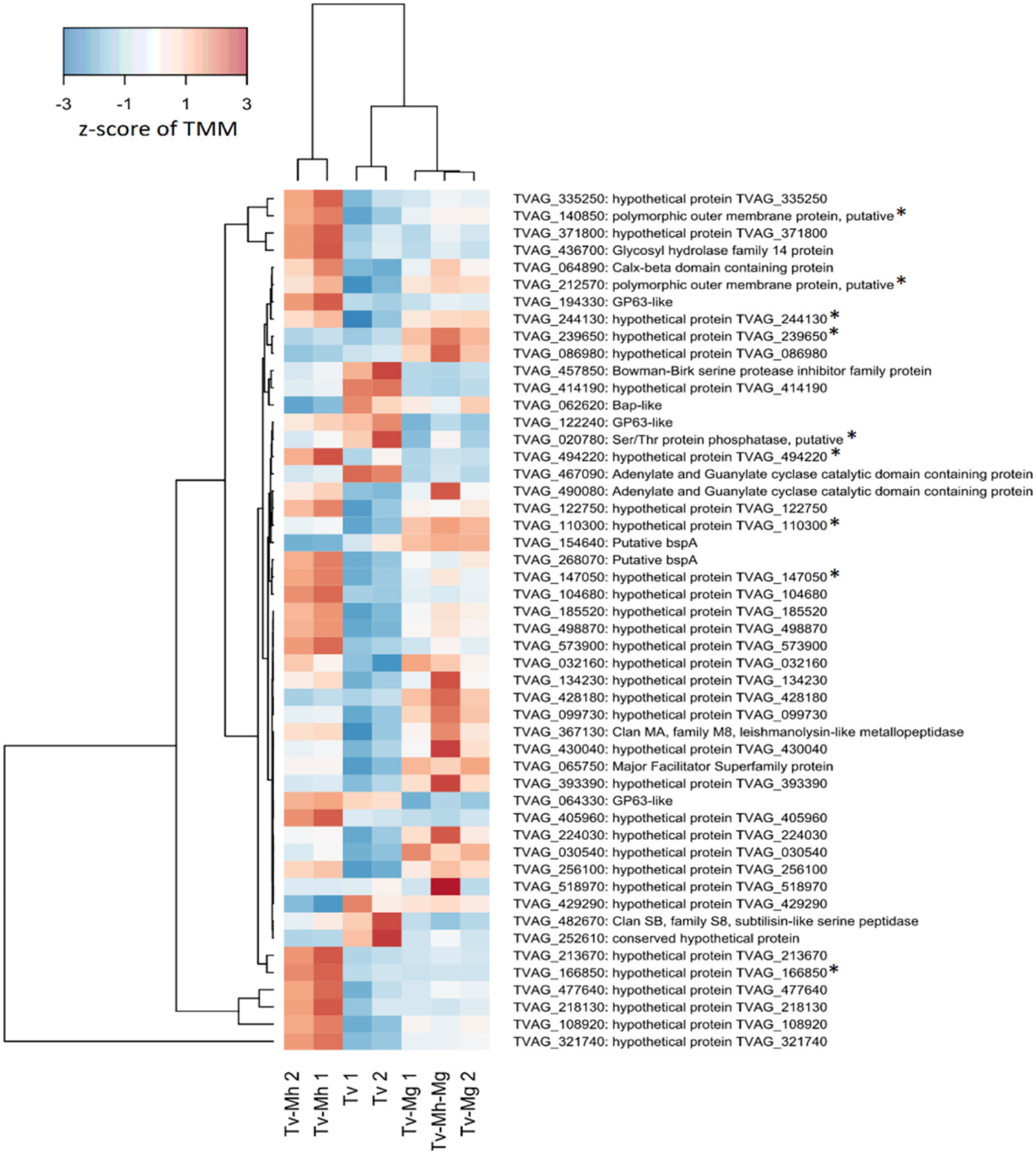

FIG 14 Differential expression of *T. vaginalis* surface protein-coding genes during coculture with *Mycoplasma*. A heatmap of experimentally verified surface protein-coding genes (54) with the top 50 lowest *P* values for differential expression under any *Mycoplasma* condition is shown. Expression units are z-scaled TMM. Genes with significantly increased abundance among more adherent *T. vaginalis* strains (54) are marked with an asterisk.

***Mycoplasma* in symbiosis with *T. vaginalis* increases both parasite hemolytic properties and adherence to human epithelial cells.** The observed significant influence of "*Ca.* M. girerdii" and *M. hominis* on the transcriptome of the protist led us to evaluate with two different cell-based assays the potential modulation of the two *Mycoplasma* species on the pathobiology of the parasite. Using a hemolysis assay (60),

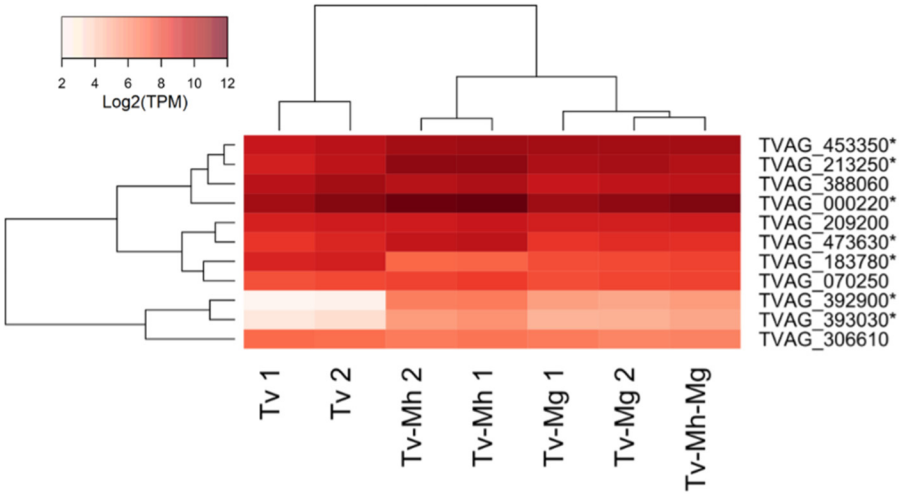

FIG 15 Heatmap of genes encoding saposin-like (TvSAPLIP) proteins significantly differentially expressed under TvSS-62iso+Mh, TvSS-62Mg, and TvSS-62Mg+Mh conditions versus the TvSS-62iso condition. The heatmap shows 7 out of the 11 transcripts encoding candidate TvSAPLIP proteins significantly differentially expressed under TvSS-62iso+Mh (Tv-Mh), TvSS-62Mg (Tv-Mg), and TvSS-62Mg+Mh (Tv-Mh-Mg) conditions versus the TvSS-62iso condition. Expression is shown in units of $\log_2$ transcripts per million (TPM).

we examined the amount of hemoglobin released by human erythrocytes (RBCs) upon contact with TvSS-62iso (mycoplasma-free *T. vaginalis*), TvSS-62Mg (*T. vaginalis* naturally infected by "*Ca.* M. girerdii"), and TvSS-62Mg+Mh (*T. vaginalis* experimentally infected by *M. hominis*) over three time points, 90, 120, and 180 min. Similar to the data for *T. vaginalis* strain G3 associated with *M. hominis* (22), the protists infected by "*Ca.* M. girerdii" and with double infection were both characterized by higher hemolytic activities than for the mycoplasma-free isogenic *T. vaginalis* strain at the 180-min time point ($P < 0.05$) (Fig. 17).

In agreement with the *Mycoplasma*-associated significantly increased amounts of transcripts for a number of genes encoding surface proteins mediating binding to the

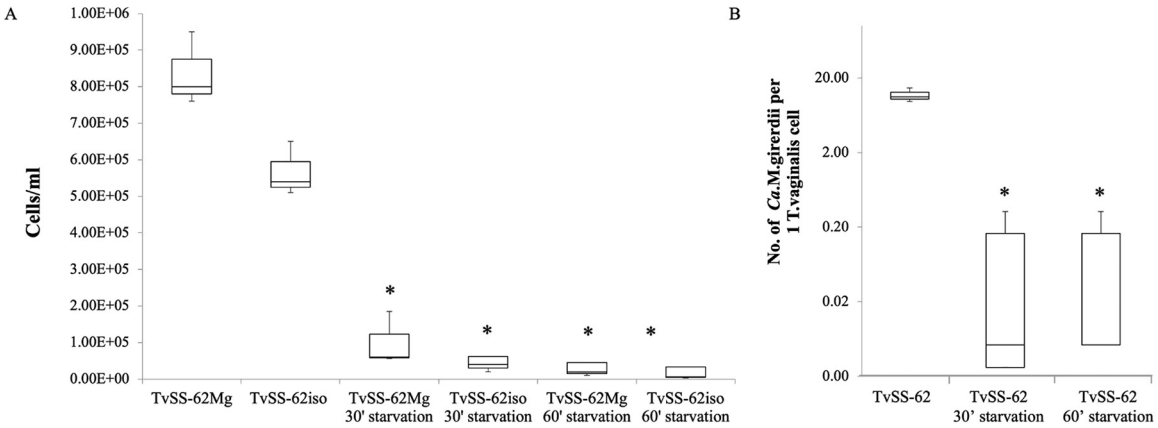

FIG 16 Impact of nutritional stress on *T. vaginalis*-"*Ca.* M. girerdii" symbiosis. (A) Cultures from isolate TvSS-62Mg (naturally infected with "*Ca.* M. girerdii") and TvSS-62iso (experimentally cleaned from "*Ca.* M. girerdii") were grown in complete medium for 24 h, used as controls for comparison with TvSS-62Mg and TvSS-62iso exposed to PBS for either 30 min or 60 min, and then grown for 24 h in complete medium, and counts of *T. vaginalis* cells were performed from triplicates. Data were analyzed by Student's *t* test, and * indicates a *P* value of <0.05 for *T. vaginalis* cultures exposed to normal medium compared to cells exposed for 30 or 60 min to PBS. (B) The impact of the TvSS-62Mg symbiosis exposed to control or PBS medium on the MOI of "*Ca.* M. girerdii" in *T. vaginalis* was measured by qPCR on the set of samples shown in panel A. Either starvation condition massively decreased the mean MOI value of "*Ca.* M. girerdii" in trichomonad cells compared with the control, indicating a high sensibility of the bacteria to the tested environmental change. Bars represent the means ± SD, and the boxes represent the number of *T. vaginalis* cells in 1 mL of culture (A) and the number of "*Ca.* M. girerdii" bacteria per 1 trichomonad cell (B) from three independent growth experiments. Statistical significance was tested by Student's *t* test, and * indicates significant ($P < 0.05$) variations in terms of the mean MOI value of "*Ca.* M. girerdii" per *T. vaginalis* cell.

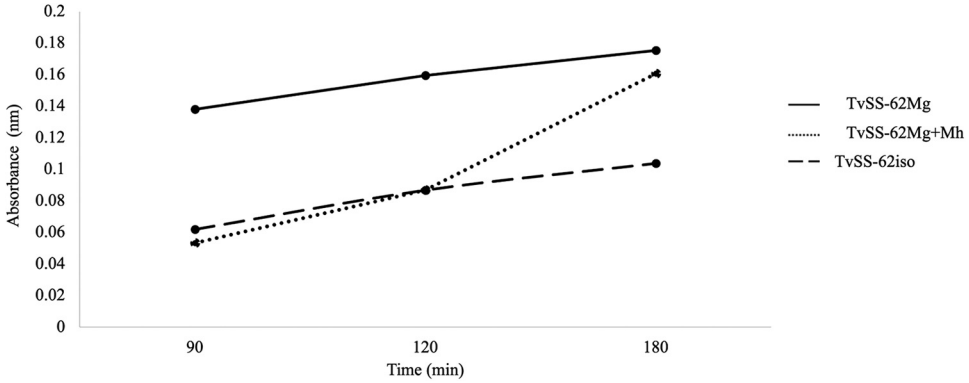

FIG 17 Influence of *Mycoplasma* species on the hemolytic activity of *T. vaginalis*. The hemolytic activity exerted by "*Ca*. M. girerdii" alone and associated with *M. hominis* in *T. vaginalis* SS-62 was compared with that of *T. vaginalis* SS-62iso (experimentally cleaned from "*Ca*. M. girerdii"), evaluating hemoglobin released by human RBCs through spectrophotometric analysis (reading at a 546-nm absorbance). The values are expressed as hemoglobin released by RBCs upon contact with pathogens and represent averages and standard deviations (error bars) from three independent experiments. Statistical significance was investigated by Student's *t* test, and * indicates significant ($P < 0.05$) variations compared to parasites without *Mycoplasma* species.

host cell (48), parasite binding to human NOK and HeLa cells after a 30-min incubation was significantly upregulated (~10-fold) in the presence of either *Mycoplasma* species, or the combination, compared to the isogenic strain TvSS-62iso (Fig. 18).

These results support the hypothesis suggested by the RNA-Seq data that the presence of *M. hominis* and "*Ca.* M. girerdii" influences positively both the capacities for *T. vaginalis* hemolysis and adhesion to host epithelial cells, two important features of *T. vaginalis* pathobiology (33, 54, 60).

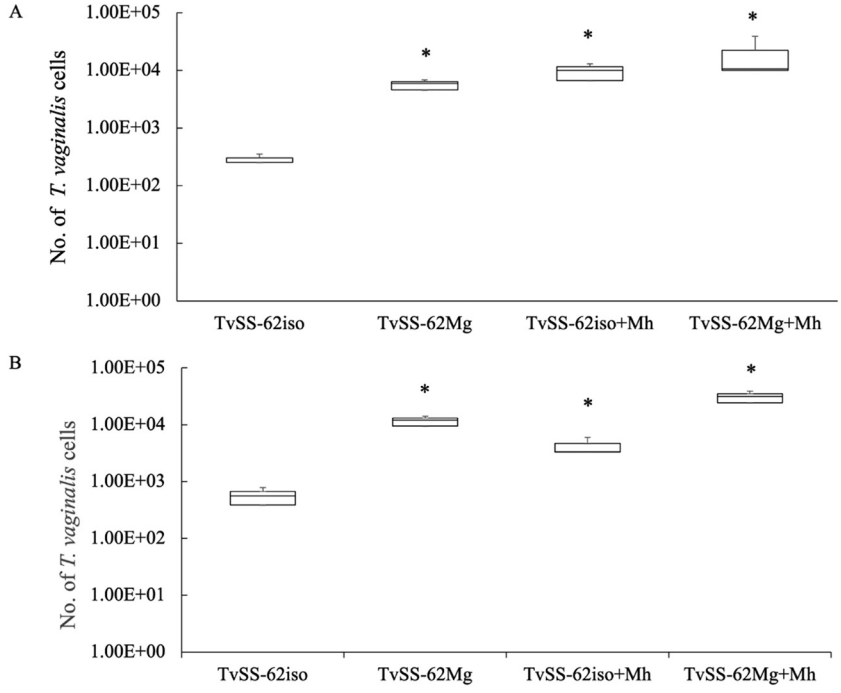

FIG 18 *Mycoplasma* increases the adherence of *T. vaginalis* to epithelial cells. Adherence to NOK cells (A) and HeLa cells (B) of *T. vaginalis* isogenic strains (TvSS-62iso, experimentally mycoplasma cleaned; TvSS-62Mg, naturally "*Ca*. M. girerdii" infected; and TvSS-62iso+Mh and TvSS-62Mg+Mh, experimentally infected by *M. hominis*) was evaluated, and the number of trichomonad cells attached to epithelial cells after a 30-min incubation was determined by qPCR. Data obtained from two experiments performed in triplicate show that the presence of "*Ca*. M. girerdii" and *M. hominis* in *T. vaginalis* statistically influences adhesion, increasing the number of cells attached to the monolayer (*, $P < 0.05$).

DISCUSSION

The ability of *T. vaginalis* to act in concert with endosymbiotic bacteria and viruses in the vaginal environment is an intriguing aspect of protozoan pathobiology (13, 21, 33, 61) and represents a fascinating and unique case of comorbidity from distinct microbes involved in different combinations of endosymbiosis, which can involve various combinations of up to two *Mycoplasma* species and up to four TVVs. Notably, multimorbidities are increasingly recognized to represent significant contributors to both mortality and morbidity rates during pregnancy (34), and the acquisition of *T. vaginalis* during gestation represents an additional risk for adverse pregnancy outcomes (61, 62). The parasite-*Mycoplasma*-TVV consortia could activate an excessive inflammatory response upon the release of TVV virions and *Mycoplasma* cells (21) after treatment with metronidazole, potentially complicating the outcome of pregnancy (15, 20, 21, 63). Furthermore, metagenomic investigations and 16S rRNA microbial surveys have shown that several vaginal bacterial communities are associated with trichomoniasis (26, 27, 64). The vaginal microbiota of women with trichomoniasis is characterized by an abundance of *M. hominis* (20, 61) and by the presence of an uncultured bacterium named "*Ca.* M. girerdii" (26, 27). In the current study, we developed an *in vitro* model of coinfection demonstrating the endosymbiotic nature of the relationship between the two *Mycoplasma* species and *T. vaginalis*.

Epidemiological data on "*Ca.* M. girerdii" analyzed in this work identified a prevalence of 61% among clinical *T. vaginalis* isolates derived from vaginal swabs from 75 Italian patients affected by acute trichomoniasis. This was consistent with the previously published prevalence of 44% (63 patients) to 63% (30 patients) for "*Ca.* M. girerdii" in vaginal samples of women clinically diagnosed with trichomoniasis in the United States (26, 27). A BLASTN search of the NCBI database with the 16S rRNA gene from "*Ca.* M. girerdii" (strain VCU_M1) identified hits with 100% identity from sequences resulting from various vaginally derived samples from China (e.g., GenBank accession numbers LC272065.1 and LC554418.1), and more recently, cultures of *T. vaginalis* associated with either of the mycoplasma species investigated were also characterized from *T. vaginalis* clinical isolates from Chinese patients (39). These different data suggest that the presence of "*Ca.* M. girerdii" is likely to be observed worldwide and is likely relevant for *T. vaginalis*-infected patients across most, including Caucasian, African-American, and Han people, if not all, ethnic groups across the globe.

Notably, our study shows that *T. vaginalis* is rarely uniquely associated with "*Ca*. M. girerdii" as 56% of *T. vaginalis* clinical isolates are naturally associated with both "*Ca.* M. girerdii" and *M. hominis*, with only 5% of *T. vaginalis* isolates analyzed in this work being associated with "*Ca*. M. girerdii" alone. Moreover, only 11% of *T. vaginalis* isolates from the investigated cohort of patients from Italy were mycoplasma free. Consistent with these data, a broad 16S rRNA gene survey on vaginal swabs from mainly African-American women (27) also identified both mycoplasma species from the same patient, with the majority (67%) of *T. vaginalis* infections associated with one or both mycoplasma species, indicating that the *T. vaginalis* association with "*Ca*. M. girerdii" and/or *M. hominis* is globally distributed across communities. These data strongly support the hypothesis that *T. vaginalis* is able to establish a stable relationship with "*Ca*. M. girerdii" alone and in association with *M. hominis*. Furthermore, this symbiosis might be more robust *in vivo* since based on the 16S rRNA survey data, "*Ca*. M. girerdii" was shown to be able to dominate the bacterial portion of the vaginal microbiome in the presence of *M. hominis* and *T. vaginalis* (27) (Fig. 1).

These results led us to investigate the MOIs of "*Ca.* M. girerdii" among different *T. vaginalis* isolates and to evaluate whether the presence of one mycoplasma species might influence the other under controlled *in vitro* growth conditions. Our data based on quantitative real-time PCR demonstrated that the ratio of "*Ca*. M. girerdii" to trichomonad cells in four isolates ranged from 4:1 to 18:1 (mean, 11:1) when "*Ca*. M. girerdii" is associated exclusively with *T. vaginalis*. Notably, in all *T. vaginalis* isolates in symbiosis grown *in vitro* with both mycoplasmas, the estimated MOI of "*Ca*. M. girerdii" per

trichomonad cell was significantly lower (mean value of 1:19 bacteria per *T. vaginalis* cell). This was in contrast to the proportion of reads that mapped to 16S rRNA genes in vaginal swabs, with the majority of samples characterized by a majority of reads attributed to "*Ca*. M. girerdii" compared to *M. hominis* in *T. vaginalis*-infected patients (Fig. 1; see also Table S1 in the supplemental material) (27). While there are biases in proportional data from 16S rRNA surveys (41, 65), this suggests at face value that the biomass of "*Ca*. M. girerdii" is typically higher than that of *M. hominis* when both bacteria are present in *T. vaginalis*-infected women (Fig. 1B and D). Considering that both mycoplasmas are predicted to easily lyse, the sequences of the 16S rRNA genes targeted by the primers used to amplify the V1-V3 hypervariable regions from "*Ca*. M. girerdii" and *M. hominis* are identical to each other, and *M. hominis* strains typically have two 16S rRNA genes, in contrast to the single 16S rRNA gene in "*Ca*. M. girerdii," these PCR-based data are consistent with a higher biomass of "*Ca*. M. girerdii" than of *M. hominis* in *T. vaginalis*-infected women. Consistent with the 16S rRNA survey of the vaginal microbiota, the proportions of mRNA-derived reads between the two *Mycoplasma* species in the *in vitro* cultures indicated a higher biomass for "*Ca*. M. girerdii" than for *M. hominis*. However, for all the native cultures of isolates with dual mycoplasma species, the MOI was inconsistent with this picture, with an opposite trend in their respective MOIs. This could be explained by the use of the TvSS-62–"*Ca*. M. girerdii" pair, the native symbiosis, where both partners may have adapted to each other. Variations observed between the *in vitro*- and *in vivo*-derived data could be due to variations in the concentrations of key metabolites in Diamond's TYM medium and vaginal fluid/surfaces, respectively, with notably arginine being typically characterized by lower concentrations among BV patients (9). Such variations in metabolites could differentially impact the growth capabilities of "*Ca*. M. girerdii" versus *M. hominis* as arginine is known to represent the major source of energy for the latter but is unlikely to be relevant as an energy source for the former, which can use glycolysis based on genome annotation (27). The observed variation of MOIs for *M. hominis* measured by qPCR was consistent with previous data where *T. vaginalis* displays important isolate-to-isolate variability for *M. hominis* MOIs among clinical isolates as estimated by semiquantitative assays (47). All these data support the hypothesis that the capability of infection of "*Ca*. M. girerdii" may be inhibited by the presence of *M. hominis*, leading us to speculate on the existence of some form of competition between *M. hominis* and "*Ca*. M. girerdii" when in dual symbiosis with *T. vaginalis*. This hypothesis is also supported by our data obtained using our experimental infection model, which show that while "*Ca*. M. girerdii" can readily infect the axenic *T. vaginalis* recipient, the infection is much more difficult, if not impossible, when "*Ca*. M. girerdii" must infect *T. vaginalis* stably associated with *M. hominis* or when the two species of mycoplasma are coincubated with a mycoplasma-free parasite recipient. In the latter case, *T. vaginalis* establishes a stable relationship with *M. hominis* only, while "*Ca*. M. girerdii" is eliminated after a few days of cultivation. Moreover, we have observed the instability of the symbiosis between naturally mycoplasma-free *T. vaginalis* and "*Ca*. M. girerdii," hypothesizing that such instability could be due to intrinsic difficulties of the naturally mycoplasma-free protist, potentially due to a lack of adaptation between the parasite and "*Ca*. M. girerdii." These different considerations suggest complex metabolic interactions.

In order to evaluate the robustness of the "*Ca*. M. girerdii"-*T. vaginalis* association to some environmental changes, we performed starvation experiments with TvSS-62Mg, naturally in symbiosis with "*Ca*. M. girerdii," and TvSS-62iso, experimentally cleaned from mycoplasmas. Upon short (30- and 60-min) starvation in PBS, the MOI of "*Ca*. M. girerdii" drastically decreases from ~12 bacteria per parasite in TvSS-62Mg to ~1 bacterium per trichomonad, indicating that unfavorable environmental conditions can strongly influence the ability of "*Ca*. M. girerdii" to infect the parasite or the parasite's capacity to host the bacteria. These data were further supported by the results obtained by limiting dilution experiments assessed for TvSS-62Mg, where we detected genomic DNA of "*Ca*. M. girerdii" until a dilution of 12.5 *T. vaginalis* cells seeded per

well in 100 μL of medium. This could be due to increased xenophagy of the bacteria by the parasite in response to this stress, as autophagy is known to be stimulated in *T. vaginalis* by glucose starvation (66). Alternatively, this could be due to the stress directly impacting the bacteria or a combination of these two processes.

The "*Ca.* M. girerdii"-*T. vaginalis* symbiosis is likely to be based on different metabolic interactions compared to the *M. hominis*-*T. vaginalis* consortium given the fundamentally different bases of energy metabolism identified for these two mycoplasma species: glycolysis in "*Ca.* M. girerdii" (27) and amino-acid-based (arginine) metabolism in *M. hominis* (24, 35). The *T. vaginalis*-*M. hominis* symbiosis brings together two ADH pathways exhibiting increased arginine consumption, concomitant with increases in ornithine and putrescine production (24). Notably, the addition of free arginine to culture medium is associated with an increase in the amount of ATP/cell in the *T. vaginalis*-*M. hominis* consortium, suggesting cross-beneficial metabolic interactions between the two symbiotic partners (22). Moreover, a recent study showed that under glucose restriction, *T. vaginalis* rapidly consumes arginine from the medium to generate ATP with a slight increase in proline levels (66). These findings support a model where the presence of *M. hominis* could help and promote the growth of *T. vaginalis* and could explain the higher MOI for *M. hominis* than for "*Ca*. M. girerdii" in *T. vaginalis* strains with double infection grown in TYM medium.

Another interesting finding was the demonstration of the intracellular localization of "*Ca.* M. girerdii" in *T. vaginalis* cells, given that previous fluorescence *in situ* hybridization (FISH) data rarely showed the bacteria colocalizing with *T. vaginalis* (27). Through a gentamicin protection assay, we found that the bacteria associated with *T. vaginalis* cells can survive under antibiotic exposure for 15 days. Notably, the number of bacteria associated with *T. vaginalis* cells was not statistically significantly different in parasites cultivated in the presence or absence of gentamicin (Table S7). Moreover, the intracellular location was further supported by fluorescence assays in *T. vaginalis* after cultivation in medium supplemented with gentamicin. The microscopy and qPCR data suggest that "*Ca.* M. girerdii" can live both on the cell surface and in an intracellular compartment in *T. vaginalis* cells, with a higher number of cells in the latter compartment. These data in combination thus suggest that the replication of "*Ca.* M. girerdii" in this system occurs mainly intracellularly, in contrast to *M. hominis*, which, even if it is able to multiply in the parasite cytoplasm, can also replicate, and substantially so, extracellularly under the tested *in vitro* growth conditions (45). These considerations are also consistent with the inability to grow "*Ca*. M. girerdii" *in vitro* despite numerous attempts (27).

We have also performed comparative growth experiments to determine whether "*Ca*. M. girerdii" can influence parasite multiplication by studying the growth kinetics of *T. vaginalis* alone or coinfected with one or both mycoplasma species: *T. vaginalis* cultures associated with either mycoplasma or with both bacterial species promoted the parasite growth rate. The observed mycoplasma-dependent boost in *T. vaginalis* growth supports a model in which all three microbial species synergistically promote their respective survival and growth *in vivo*.

These results are also supported by the *in vitro* RNA-Seq analyses of *T. vaginalis* experimentally cleaned from "*Ca.* M. girerdii" (TvSS-62iso), *T. vaginalis* naturally associated with "*Ca.* M. girerdii" (TvSS-62Mg), *T. vaginalis* experimentally infected by *M. hominis* (TvSS-62iso+Mg), and doubly infected *T. vaginalis* (TvSS-62Mg+Mh). Consistent with the increase in the growth rate of *T. vaginalis* in symbiosis with *M. hominis* (22) and "*Ca*. M. girerdii," RNA-Seq analyses indicated a major upregulation of *T. vaginalis* functions related to central energy metabolism and the storage of glycogen and a corresponding response to the potentially resultant increase in redox stress. Interestingly, the differential expression of central energy metabolism genes suggested a shift from hydrogenosomal metabolism toward cytosolic lactate and malate fermentation. Increased lactate dehydrogenase (LDH) expression may deplete pyruvate as a hydrogenosomal substrate, and hydrogenosomal malate consumption may be reduced by decreased malic enzyme expression (67). The significance of this shift is unclear, but synergistic *Trichomonas-Mycoplasma* metabolism could

compensate for the loss of energy usually derived from substrate-level phosphorylation in the hydrogenosome. Alternatively, it was suggested previously by Westrop et al. (68) that some *T. vaginalis* LDH enzymes are involved in 2-hydroxy acid synthesis. As 2-hydroxy acids can inhibit microbial growth, it is possible that this response functions to limit *Mycoplasma* growth or to compete with other mucosal microorganisms *in vivo*. Increased amino acid catabolism may also have provided energy and biomass to support growth. The ADH pathways for energy generation shared by *T. vaginalis* and *M. hominis* suggest a potential synergistic metabolism. However, our transcriptional results concerning the ADH pathway are unclear. Overall, most enzymes showed little modulation in response to *Mycoplasma*. The influence of the opposite regulatory profiles of the 2 OCT homologs is difficult to interpret. Experimental characterization would be required to determine whether sequence differences between these proteins influence activity or posttranslational regulation. Interestingly, genes putatively annotated as arginase genes were upregulated in the presence of *Mycoplasma*. Previous evidence suggests that *T. vaginalis* cells lack arginase activity, although these experiments were likely conducted in the absence of both *M. hominis* and "*Ca.* M. girerdii" (69). Arginase could allow *T. vaginalis* to outcompete *M. hominis* for arginine to allow the continued synthesis of putrescine necessary for cell survival (68, 70, 71).

Ribosome biogenesis, a defined marker of an increased growth rate (72), was also increased in the presence of "*Ca*. M. girerdii" at the mRNA level.

The RNA compositional results between samples suggested an overall greater biomass of "*Ca.* M. girerdii" than of *M. hominis*, which may be consistent with the observed increase in expression at the mRNA level of lysosomal proteins specifically during symbiosis with *M. hominis*, which has also been observed in human cells infected with *M. hominis* (73). This may be involved in destroying some of the intracellular bacteria (45) through xenophagy, as was suggested previously by Vancini and Benchimol for *T. vaginalis* in symbiosis with *M. hominis* (44). These observations are congruent with a preference for the natural "*Ca*. M. girerdii" symbiont of the *T. vaginalis* strain (TvSS-62Mg) used for these experiments, as has been observed for other eukaryote-bacterium symbioses (74). In triple culture, "*Ca.* M. girerdii" appeared to outcompete *M. hominis* but also benefited from its presence in terms of its own abundance. Consistent with this, "*Ca.* M. girerdii" appeared to be the main driver of differential gene expression during the simultaneous symbiosis of *T. vaginalis* with *M. hominis*, as the expression profile under this condition most closely resembled that of the individual *T. vaginalis*-"*Ca.* M. girerdii" symbiosis and was distinct from that of *T. vaginalis* in symbiosis with *M. hominis*. Surprisingly, despite the major differences in the metabolic configurations between *M. hominis* and "*Ca.* M. girerdii," there is a largely overlapping transcriptional response in *T. vaginalis* cells in symbiosis with these *Mycoplasma* species, including many common metabolic functions. We hypothesize that this may result from transcriptional regulation by *Trichomonas* in response to biochemical features common to both *Mycoplasma* species, such as their lipids.

Mycoplasma has been reported to influence various processes potentially related to *T. vaginalis* mucosal colonization and pathogenesis (22, 25, 75), which was reflected in our findings. The TvBspA-like gene family has been massively expanded, with over 900 members (37), substantial proportions of which were differentially expressed (255 genes) in response to the different symbioses with *Mycoplasma*. This potentially implicates the presence of *Mycoplasma* as a trigger to modulate host and *T. vaginalis*-microbe adhesion, particularly in the case of surface-localized TvBspA-like proteins verified by proteomics and other means (37, 54). Typically, LRR motifs are thought to facilitate protein-protein interactions (57), so TvBspA-like proteins may also play various roles in interactions with other cells, including host cells (53) and other microbes, such as the mycoplasmas themselves, and more generally could mediate binding to members of the microbiota that the parasite is known to bind to and phagocytose (76, 77). In support of this, we observed a complex regulatory pattern across the TvBspA-like gene family, with some genes being specifically upregulated in response to a single *Mycoplasma* species, suggesting a role in species-specific *Trichomonas-Mycoplasma*

interactions. BspA-like genes were simultaneously expressed at a high level by "*Ca.* M. girerdii," potentially providing a cognate interaction partner with the TvBspA-like protein, as demonstrated for BspA-like proteins from different species of oral bacteria (36).

In strong support of a host adhesion regulatory role of *Mycoplasma*, the majority, 8 of the 11 *T. vaginalis* genes, for which the corresponding proteins showed increased expression on the surface proteomes of more highly adherent *T. vaginalis* strains (54), were significantly upregulated at the mRNA level in response to the presence of *Mycoplasma*. Notably, higher levels of transcription of such genes were shown to be associated with higher levels of surface protein expression (54).

These data led us to investigate *in vitro* the influence of both mycoplasmas on two important aspects of *T. vaginalis* cytopathogenicity. In particular, we have assessed the ability of *T. vaginalis-Mycoplasma* consortia to lyse human RBCs compared with *T. vaginalis* alone: our data showed that both mycoplasma species were able to enhance the protozoan cytolytic effect, confirming our previous results on the impact of *M. hominis* endosymbiosis on the parasite hemolytic effect (22). We also evaluated the adherence capacity of *T. vaginalis* associated with one or both *Mycoplasma* species compared with *Mycoplasma*-free *T. vaginalis* on the basis of RNA-Seq results: our data demonstrate that the number of protist cells attached to epithelial cells was ~10-fold higher when symbiotically associated with one or both *Mycoplasma* species than with *T. vaginalis* alone.

A final consideration concerned oxidative stress tolerance, which is implicated in the virulence of various pathogens by providing resistance to ROS-mediated killing by immunocytes (78). Thus, the observed increase in ROS detoxification enzymes in response to *Mycoplasma* endosymbiosis could also be implicated in *T. vaginalis* pathobiology. This may work in synergy with another mechanism of tolerance mechanism to immunocyte-derived ROS thought to be facilitated by *M. hominis* via the catabolic depletion of arginine, the substrate for nitric oxide production (22).

This work highlights for the first time the stable intracellular relationship that "*Ca.* M. girerdii" forms with *T. vaginalis* and shows the ability of *M. hominis* to play a pivotal role in the relationships with the new mycoplasma species strictly associated with the parasite. The existence of such strongly intertwined microbial relationships in specific ecological niches in the human body depicts a picture of complex interactions between different microorganisms with pathogenic potential. Taken together, these findings support a model in which associations between *T. vaginalis* and vaginal mucosal bacteria are likely to influence and contribute to the broad diversity of the health sequelae associated with trichomoniasis. Future investigations should consider evaluating *T. vaginalis*-positive patients in combination with their *Mycoplasma* and TVV symbiosis status to determine whether such stratification could effectively predict a higher risk for preterm birth and/or HIV transmission/acquisition. Such patient stratifications would also have important implications for diagnostics, which could benefit from simultaneously detecting parasites, bacteria, and TVVs (21, 61).

MATERIALS AND METHODS

Analysis of published 16S rRNA data. Previously published 16S rRNA data from mid-vaginal swab samples (27) were reanalyzed under study HM12169 as approved by the institutional review boards for human subject protection at the Virginia Commonwealth University and the Virginia Department of Health. Briefly, the V1-V3 hypervariable regions of the 16S rRNA gene were amplified using primers with a sequencing adaptor (shown in italics), a 6- to 9-base variable barcode sequence, and the 5′ end of the primer. The forward primer was a 4:1 mixture of primers Fwd-P1 (5′-*CCATCTCATCCCTGCGTGTCTCCGACTCAG*BBBBBBAGAGTTYGATYMTGGCTYAG) and Fwd-P2 (5′-*CCATCTCATCCCTGCGTGTCTCCGACTCA*GBBBBBAGARTTTGATCYTGGTTCAG). The reverse primer was Rev1B (5′-CCTATCCCCTGTGTGCCTTGGCAGTCTCAGATTACCGCGGCTGCTGG).

PCR products were sequenced on the Roche 454 GS FLX Titanium platform. Sequencing reads with a valid primer and barcode were retained for analysis if they had fewer than 10% of base calls with a quality score of less than 10, an average quality score of greater than Q_{20}, and a read length of between 200 and 540 bases. All analyzed samples had more than 5,000 reads. Taxonomic classification was performed using STIRRUPS (79). The analyzed data sets included profiles of 63 samples collected at the time of a trichomoniasis diagnosis and 73 women with detection of "*Ca.* M. girerdii" at 0.1% of the overall 16S

rRNA profile. Among the 63 women with trichomoniasis, 28 samples had "*Ca.* M. girerdii" at 0.1%, 26 of which were available for inclusion in the group of 73 women with "*Ca.* M. girerdii."

Culture conditions for *T. vaginalis* and *Mycoplasma* species. A total of 75 *T. vaginalis* strains previously isolated in the laboratory of microbiology of the University of Sassari from Italian female patients affected by acute trichomoniasis were investigated for the presence of *M. hominis* and "*Ca.* M. girerdii." *T. vaginalis* strains were cultivated by daily passage at 1:16 in Diamond's TYM (Trypticase, yeast extract, and maltose) medium supplemented with 10% fetal bovine serum (FBS) at 37°C in a 5% CO_2 atmosphere (80) for 2 weeks. Genomic DNA was extracted with a commercial kit, the DNeasy blood and tissue kit (Qiagen Ltd., West Sussex, UK), according to the manufacturer's protocols and analyzed by quantitative real-time PCR (qPCR).

A total of three *T. vaginalis* isolates were used for generating isogenic strains: *T. vaginalis* reference strain G3 (TvG3), naturally mycoplasma free; *T. vaginalis* strain SS-62 (TvSS-62Mg), naturally "*Ca.* M. girerdii" infected; and *T. vaginalis* strain SS-25 (TvSS-25MgMh), naturally associated with both *M. hominis* and "*Ca.* M. girerdii."

M. hominis cells were isolated from *T. vaginalis* strain TvMPM2, which is naturally associated with *M. hominis* (47), and maintained in BEA medium (2.2% heart infusion broth, 15% horse serum, 1.9% yeast extract, 40 IU/mL benzylpenicillin, 0.23% L-arginine, 0.0023% phenol red [pH 7.2]) (81).

"*Ca*. M. girerdii" has not been isolated and maintained in culture in the absence of *T. vaginalis* despite several attempts to do so (27). In our experiments, we used bacteria from the supernatant of naturally "*Ca.* M. girerdii"-infected TvSS-62Mg cultures to experimentally infect mycoplasma-free and *M. hominis*-infected *T. vaginalis* strains.

Quantitative real-time PCR assay for MOI determination. qPCR assays for "*Ca.* M. girerdii" and *M. hominis* were performed using the CFX96 Touch real-time thermal cycler (Bio-Rad, Hercules, CA). Absolute quantification of "*Ca.* M. girerdii" and *M. hominis* DNA concentrations was performed by serial dilution of plasmids containing a single-copy housekeeping gene sequence. For "*Ca.* M. girerdii," the full-length 16S rRNA gene cloned into pCR 2.1-TOPO was used as the standard. For *M. hominis*, a fully conserved gene fragment of a surface lipoprotein with nuclease activity (82), MHO_0730 (*M. hominis* strain ATCC 23114) cloned into pGEX2T, was used as the template to generate a standard curve. The primer sets used are listed in Table 5. The PCR mixture consisted of 2× SYBR select master mix (Applied Biosystems), 300 nM each primer, 10 to 100 ng/mL of the genomic DNA sample, and nuclease-free water (Invitrogen) to a volume of 20 μL.

For "*Ca.* M. girerdii," amplifications were performed for 2 min at 50°C and 10 min at 95°C, followed by 40 cycles of 15 s at 95°C and 1 min at 60°C. After the real-time PCR amplification was completed, a melting analysis was performed. The samples were heated to 95°C for 1 min, cooled to 60°C (0.10°C/s), and reheated to 95°C (0.5°C/s).

For *M. hominis*, the PCR program used was 2 min at 50°C and 10 min at 95°C, followed by 40 cycles with denaturation at 95°C for 15 s and annealing and elongation at 60°C for 1 min. After PCR, a melting program finalized the analysis.

Each sample was tested in triplicate, and negative and positive controls were processed in parallel in the same experiment.

Gentamicin susceptibility of "*Ca.* M. girerdii" in symbiosis with *T. vaginalis*. "*Ca.* M. girerdii"-infected TvSS-62Mg bacteria were cultivated in Diamond's TYM medium supplemented with 50 μg mL^{-1} gentamicin. Aliquots of the culture were taken at different times (after 1, 3, 7, and 15 days of incubation with gentamicin) to assess long-term intracellular survival. Cells were centrifuged at 500 × *g* for 10 min; the cellular pellet was extensively washed in phosphate-buffered saline (PBS) three times and, together with the supernatant, was subjected to total DNA extraction as described above. Detection of "*Ca.* M. girerdii" DNA in the supernatant or associated with *T. vaginalis* whole cells was performed by qPCR. Furthermore, the presence of "*Ca.* M. girerdii" within trichomonad cells after 15 days of gentamicin treatment was investigated by fluorescence microscopy, staining the cells with 5 μg/mL DAPI (4′,6-diamidino-2-phenylindole) (see below). The supernatant from TvSS-62Mg cultures treated for 15 days was used to infect mycoplasma-free TvG3 in order to evaluate the residual ability to infect mycoplasma-free recipients. "*Ca*. M. girerdii"-infected TvSS-62Mg bacteria cultivated in Diamond's TYM normal medium were used as controls.

Experimental model to study the ability of *Mycoplasma* to infect *T. vaginalis*. Isogenic *T. vaginalis* cultures were obtained by using two different approaches: (i) naturally mycoplasma-free TvG3 cells were infected with *M. hominis* or "*Ca.* M. girerdii" (24), or (ii) mycoplasma-infected strains TvSS-62Mg and TvSS-25MgMh were cleared of native mycoplasmas using Plasmocin (InvivoGen) as previously described (48). Mycoplasma-free *T. vaginalis* strains were subsequently used as the recipients and infected with the two *Mycoplasma* species in either single or double infections.

For the first approach, in order to obtain TvG3 stably infected with either *M. hominis* or "*Ca.* M. girerdii," we collected the supernatants of TvMPM2Mh (naturally infected by *M. hominis*) or TvSS-62Mg (naturally infected by "*Ca.* M. girerdii") by centrifuging cell cultures at 350 × *g* for 10 min. The supernatants containing 1.09E+05 *M. hominis* or 2.07E+06 "*Ca.* M. girerdii" cells, quantified based on qPCR, were filtered using a 0.22-μm-pore-size filter membrane and then separately added for 3 days to 10 mL of mid-log-phase TvG3 cells. To study the ability of *M. hominis* and "*Ca*. M. girerdii" to form a symbiosis with "*Ca*. M. girerdii"- or *M. hominis*-containing *T. vaginalis*, respectively, *M. hominis* in symbiosis with the TvG3 strain was incubated with "*Ca.* M. girerdii," and "*Ca*. M. girerdii" in symbiosis with the TvG3 strain was incubated with *M. hominis* (Fig. 4A). Alternatively, *M. hominis* and "*Ca.* M. girerdii" were added at the same time to mycoplasma-free *T. vaginalis* cultures (Fig. 4D). Under all conditions, the different combinations of symbioses between mycoplasma and the parasite were cultivated for a further 15 days after exposure with 1:16 daily passages in Diamond's TYM complete medium, and the ability of mycoplasma

TABLE 5 Primer sequences and amplicon sizes for *M. hominis* (Mh730 forward and reverse) and "*Ca.* M. girerdii" (OTU_M1 and OTU_M2)[a]

Primer	Sequence (5′–3′)	Amplicon size (bp)	Genome positions[b]
Mh730 forward	CCAAATCCTAAACCTGGTGGT	200	101490–101690
Mh730 reverse	CGGTTCACTCCAATTGCTTGAAAT		
OTU_M1 forward	CATTTCCTCTTAGTGCCGTTCG	310	408395–408790
OTU_M1 reverse	CGGAGGTAGCAATACCTTAGC		

[a]See reference 27.
[b]Relative positions in the *Mycoplasma hominis* reference strain A136 genome (GenBank accession number CP055143.1) and "*Candidatus* Mycoplasma girerdii" reference strain UC_B3 (GenBank accession number CP020122.1).

species to establish a stable single or double symbiosis was finally tested by qPCR to quantify the amount of mycoplasma cells associated with the parasites.

For the second approach, two different clinical isolates, TvSS-62Mg, naturally in symbiosis with "*Ca.* M. girerdii," and TvSS-25MgMh, naturally in symbiosis with both "*Ca.* M. girerdii" and *M. hominis*, were treated to eliminate the endosymbiotic mycoplasmas through cultivation for 7 days in medium supplemented with Plasmocin (InvivoGen) at a final concentration of 25 μg/mL (48). Subsequently, cells were cultivated for 30 days in complete Diamond's TYM medium to obtain isogenic mycoplasma-free *T. vaginalis*, named TvSS-62iso and TvSS-25iso, respectively. The absence of bacteria was confirmed by specific qPCRs, and the influence of treatment on the replication rate of the protist was assessed by comparing the growth curve of TvSS-62iso with that of TvG3, culturing the cells for 30 days. The axenic strains TvSS-25iso and TvSS-62iso were then used as the recipients for subsequent infections, superinfections, and coinfections by *M. hominis* and/or "*Ca.* M. girerdii," as described above for the first approach. The variation of the MOI of *Mycoplasma* species in *T. vaginalis* during infection was evaluated by the extraction of DNA from aliquots of TvSS-62Mg and TvSS-62Mg+Mh cultures at 1, 7, 15, and 30 days of cultivation.

In order to avoid cross-contamination during cultivation, all isogenic parasite cultures were separately grown in different incubators and passaged daily using two different laminar flow hoods. The incubators and culture media were constantly monitored by qPCR to ensure that they were mycoplasma free.

Fluorescence microscopy. A volume of 1 mL of culture of TvSS-62Mg (naturally in symbiosis with "*Ca.* M. girerdii" and *M. hominis* free), TvSS-62iso (experimentally cleaned from "*Ca.* M. girerdii"), and TvSS-62Mg experimentally infected with *M. hominis* (TvSS-62Mg+Mh) was seeded into 24-well plates containing a round 12-mm-diameter coverslip in each well and incubated at 37°C in Diamond's TYM medium for 24 h. The cells were then gently washed with PBS (pH 7.2), fixed with 4% paraformaldehyde in PBS for 1 h, and permeabilized in 2% Triton X-100 in PBS for 2 min. Cells were then stained with 5 μg/mL DAPI to detect "*Ca.* M. girerdii" and incubated for 1 h at 37°C with anti-*M. hominis* mouse polyclonal antibodies, obtained by inoculation of total mycoplasmal proteins into mice, with subsequent elution of sera tested to validate the specific reactivity to *M. hominis* and to exclude cross-reactivity with *T. vaginalis*, as described previously by Rappelli and colleagues (47). The cells were then incubated for 30 min at 37°C with tetramethyl rhodamine isothiocyanate (TRITC)-labeled goat anti-mouse antibodies (Sigma-Aldrich) to stain *M. hominis*.

The samples were observed using an Olympus BX51 fluorescence microscope, and the images were acquired with an Optronics MagnaFire charge-coupled-device (CCD) camera.

***In vitro* multiplication rate of mycoplasma-infected *T. vaginalis* cultures and growth curve analyses.** The growth curves of four different isogenic associations, (i) mycoplasma-free *T. vaginalis* (TvSS-62iso), (ii) naturally "*Ca.* M. girerdii"-infected *T. vaginalis* (TvSS-62Mg), (iii) *M. hominis*-infected *T. vaginalis* (TvSS-62iso+Mh), and (iv) *T. vaginalis* infected by both mycoplasma species (TvSS-62Mg+Mh), were compared. Briefly, 400,000 parasite cells were inoculated into 10 mL of Diamond's TYM medium and incubated at 37°C. Cell counts were recorded at 12, 18, 24, and 36 h postinoculation. The experiments were performed three times, each in triplicate.

The growth curves for the four different *T. vaginalis* isogenic conditions (TvSS-62Mg, TvSS-62iso, TvSS-62iso+Mh, and TvSS-62Mg+Mh) were fitted in R (Growthcurver) using the standard form of a logistic equation as a function of the growth rate (r), the initial population size (N_0), and the carrying capacity (K). The equation to calculate the parasite population size (N_t) at a given time (t) is

$$N_t = \frac{K}{1+\left(\frac{K-N_0}{N_0}\right)e^{-rt}}$$

Total RNA extraction. TvSS-62Mg, naturally infected by "*Ca.* M. girerdii"; TvSS-62iso, experimentally cleaned from "*Ca.* M. girerdii"; TvSS-62Mh, experimentally infected by *M. hominis*; and *T. vaginalis* infected by "*Ca.* M. girerdii" and *M. hominis* (TvSS-62Mg+Mh) were collected in the exponential growth phase to a density of 2×10^6 cells in a final volume of 40 mL of medium. Cells were centrifuged at $500 \times g$ for 10 min, and cellular pellets were washed in 5 mL of PBS one time, resuspended in 700 μL of RNAlater (Thermo Fisher Scientific), and stored at −80°C. Material stored in RNAlater was thawed on ice, diluted with 0.7 mL nuclease-free PBS, and pelleted by centrifugation at $6{,}000 \times g$ for 5 min at 4°C. RNA was extracted from the resulting pellet using TRIzol (Thermo Fisher Scientific) according to the

manufacturer's instructions, with some modifications. Briefly, after TRIzol and chloroform were used to lyse cells and solubilize cell components, RNA was precipitated from the aqueous phase, washed, and dissolved in 25 to 30 μL nuclease-free water. After washing the RNA pellet in 75% ethanol, centrifugation at 12,000 $\times$ *g* for 10 min at 4°C was used rather than the recommended 7,500 $\times$ *g* to improve the pelleting of the RNA.

Quantification and quality analysis of RNA. The RNA concentration was determined using the Qubit RNA high-sensitivity kit (Thermo Fisher Scientific) according to the manufacturer's instructions. UV absorbance at 230 nm, 260 nm, and 280 nm was measured using a Nanodrop 2000c spectrophotometer as an indicator of purity. The absence of gDNA contamination and RNA integrity were confirmed using a TapeStation system (Agilent) by manually examining the resulting gel images and electropherograms, as the automatic RNA integrity number calculation (designed for eukaryotes) may not be suitable for mixed prokaryotic and eukaryotic total RNA.

RNA sequencing. All library preparation and Illumina sequencing were performed by Novogene UK. Libraries were prepared using a standard protocol, and prokaryotic and eukaryotic rRNAs were depleted using the Ribo-Zero kit (Illumina). Approximately 50 million paired-end reads per sample were generated using an Illumina NovaSeq 6000 platform. The read length was 150 bp, and the insert size was from 250 bp to 300 bp. Before obtaining the reads from Novogene UK, the adaptor sequences were removed, and sequences of low-quality reads (reads with >10% N's [undetermined bases] or >50% of bases at or below a Phred quality score of 5) were deleted. Sequencing data are available from the NCBI SRA database (83) under accession numbers SRR12991837 to SRR12991843.

***Trichomonas-Mycoplasma* coculture for RNA-Seq data analysis.** The workflow used to analyze gene expression from *Trichomonas-Mycoplasma* coculture RNA-Seq data is shown in Fig. S2 in the supplemental material. The average Phred quality score of all reads did not fall below 28 across the full read length as assessed by FastQC (84). Reads were filtered for rRNA sequences by alignment to a prokaryotic and eukaryotic rRNA database with SortMeRNA (49), Kraken2 was used to taxonomically assign sequences by a k-mer search against the NCBI nonredundant nucleotide database (50), and STAR was used to align reads to the reference genomes (85). SortMeRNA, Kraken2, and STAR were used with default parameters. The NCBI Taxonomy Toolkit (85) was used to agglomerate taxonomy identifications generated by Kraken2 to a specific taxonomic rank.

The *T. vaginalis* G3 genome (NCBI accession number ASM282v1) (46) was used as the parasite reference sequence, and additional annotation information was obtained for BspA-like genes from Noël and colleagues (37), for experimentally verified surface proteins (EVSPs) from the study of de Miguel and colleagues (54), and for exosomes from Twu and colleagues (55). To select the best *Mycoplasma* reference genome, *Mycoplasma* reads were aligned to available genomes from the NCBI for the corresponding species (86). *M. hominis* accession number ASM93586v1 (strain PL5) and "*Ca.* M. girerdii" accession number ASM221542v1 (strain UC_B3) were selected as showing the best alignment statistics. A decision matrix was used to compare alignment metrics for the larger number of *M. hominis* reference sequences. The overall score was calculated by multiplying the average alignment length, the percent base mismatch rate, the percentage of reads for which the alignment length was too short, the percentage of reads that did not align for other reasons, and the percentage of reads that aligned uniquely, taking the reciprocal where lower values were better, scaling values between 1 and 5, and multiplying by weights of 1, 5, 5, 10, and 10 for each metric, respectively. Genes with an expression level of at least 1 transcript per million (TPM) were considered to be expressed.

SAMtools (87) was used to manipulate alignment files. To assess sequence differences between the reference and experimental strains for genes of interest, BCftools (88) and VCFutils (89) were used to generate a consensus sequence based on the most frequent sequence variants. A *de novo* assembly of reads assigned as unclassified (ranging from 14 to 27% of the total reads) by Kraken2 was generated using rnaSPAdes (90) to investigate their identity. Reads classified as "other" (ranging from 4.3 to 8.2% of the total reads) aligned to species that were not expected to be present within the experiment. Figure S3 shows that the large majority of the assembled transcripts were short, and the mean transcript length ranged from 400 to 450 bp, which is only slightly longer than the paired-read length (300 bp).

The edgeR R package (91) was used to test for the differential gene expression of *T. vaginalis* annotated genes (46) using the negative binomial generalized linear model with a quasilikelihood test, considering only genes with a $\log_2$ fold change of greater than 1.2 for testing. Expression levels are presented as either the trimmed mean of M values (TMM) (91) or TPM, the latter calculated by the following equation:

$$\mathrm{TPM} = \frac{\text{mapped reads/transcript length}}{\sum(\text{mapped reads/transcript length})} \times 10^6$$

The TPM or z-scaled TMM was used to generate heat maps according to the range of expression of a given gene set (92).

For gene ontology (GO) enrichment analysis, PANTHER (93) was used, the full set of *T. vaginalis* genes detected to be expressed in the experiment was used as a reference database, and uninformative and redundant enriched functions were removed manually. KEGG enrichment analysis was performed using edgeR (92). For significance tests of differential gene expression and functionally enriched KEGG pathways and GO functions, *P* values were adjusted using the false discovery rate/Benjamini-Hochberg (FDR/BH) method. Testing for the differential expression of genes as a set was performed using the rotation gene set test (94) in edgeR.

A DiVenn (95) figure was created to depict the overlap of differentially expressed genes by *T. vaginalis* between the tested conditions.

KEGG metabolic pathways were predicted for "*Ca.* M. girerdii" and *M. hominis* using the online BlastKoala tool (96), using default parameters and the default reference database of prokaryotic genomes with redundancy removed at the genus level. *T. vaginalis* metabolic pathways were retrieved from the KEGG database (96).

The structural organization and cellular localization of specific proteins of interest were predicted using InterProScan (97).

Variability of "*Ca.* M. girerdii" MOIs in TvSS-62Mg under stress conditions. TvSS-62Mg, naturally "*Ca.* M. girerdii" infected, and TvSS-62iso (experimentally cleaned from "*Ca.* M. girerdii") were grown for 30 min and 60 min in PBS–1 M maltose medium, thus depriving microorganisms of a broad range of nutrients, and then cultivated for a further 24 h in complete Diamond's TYM medium. Following the starvation period, the "*Ca.* M. girerdii" MOI was calculated by using qPCR as described above. TvSS-62Mg and TvSS-62iso, normally grown for 24 h in Diamond's TYM medium and not starved, were used as controls.

Moreover, TvSS-62Mg underwent limiting dilution from 1×10^2 cells to 1 cell/well in complete Diamond's TYM medium and incubated in 96-well plates under anaerobic conditions for 10 days. DNA extraction and qPCR were performed to evaluate the presence of "*Ca.* M. girerdii" in all dilutions.

Hemolytic activity of *Mycoplasma*-infected strains. *T. vaginalis* SS-62Mg, associated with "*Ca.* M. girerdii," and *T. vaginalis* SS-62Mg+Mh, associated with both mycoplasmas, were compared with isogenic *T. vaginalis* SS-62iso, experimentally mycoplasma free, to evaluate hemolytic activity. Hemolysis assays were performed as previously described (60). Briefly, RBCs were collected from healthy human donors; erythrocytes were then washed three times in PBS and immediately used. Parasites in the exponential growth phase were washed twice in PBS and resuspended to a density of 2×10^6 cells in PBS plus 15 mM maltose (PBS-M). *T. vaginalis* isogenic strains were incubated at 37°C with washed erythrocytes at a ratio of 1:30 in PBS-M. The hemoglobin released after incubation with RBCs for different times ranging from 90 to 180 min was evaluated by spectrophotometric analysis at a 546-nm absorbance. The hemolytic capacity of "*Ca.* M. girerdii"-infected *T. vaginalis* and the doubly infected protist was compared to that of parental uninfected isogenic *T. vaginalis* SS-62iso.

Adherence assay of *T. vaginalis* isogenic strains. A *T. vaginalis* binding assay was carried out with a modified version of a method described previously (98). Briefly, oral keratinocytes (NOK) (99) and HeLa cells (ATCC CCL-2) were seeded into 24-well plates at 1.75×10^5 cells/well in culture medium and grown to confluence at 37°C with 5% CO_2 for 2 days. *T. vaginalis* isogenic strains (TvSS-62iso, TvSS-62Mg, TvSS-62Mh, and TvSS-62Mg+Mh) were added at a concentration of 10^5 cells/mL to NOK cells in triplicate. Plates were incubated at 37°C in 5% CO_2 for 30 min, and the monolayers were washed 2 times in PBS to remove unbound parasites. Subsequently, the cells (human and parasite cells with or without mycoplasma) were detached using trypsin, and DNA extraction was performed using the DNeasy blood and tissue kit. The amount of *T. vaginalis* cells bound to NOK cells was analyzed by qPCR, using actin (TVAG_534990) as a gene target.

Statistical analysis. All experiments were carried out at least in triplicate. Statistical analyses were conducted in R (100) and Microsoft Excel (Microsoft, Redmond, WA, USA) with the indicated tests. A P value of <0.05 was considered significant.

SUPPLEMENTAL MATERIAL

Supplemental material is available online only.

FIG S1, DOCX file, 0.1 MB.
FIG S2, DOCX file, 0.1 MB.
FIG S3, DOCX file, 0.1 MB.
TABLE S1, DOCX file, 0.01 MB.
TABLE S2, DOCX file, 0.02 MB.
TABLE S3, DOCX file, 0.01 MB.
TABLE S4, XLSX file, 0.01 MB.
TABLE S5, XLSX file, 0.01 MB.
TABLE S6, XLSX file, 0.1 MB.
TABLE S7, DOCX file, 0.1 MB.

ACKNOWLEDGMENT

We thank Giuseppe Delogu for the precious help in performing the microscopy assays.

This study was supported by the Biotechnology and Bioscience Research Council Doctoral Training Partnership for Newcastle, Liverpool and Durham (NPB, RPH, grant number: BB/M011186/1); by Ministero dell'Istruzione, dell'Università e della Ricerca Italy, (MIUR), grant Number 2017SFBFER_004 (PLF), and by University of Sassari, FAR 2019 (PR) and FAR 2020 (PR and PLG)

REFERENCES

1. Muzny CA, Łaniewski P, Schwebke JR, Herbst-Kralovetz MM. 2020. Host-vaginal microbiota interactions in the pathogenesis of bacterial vaginosis. Curr Opin Infect Dis 33:59–65. https://doi.org/10.1097/QCO.0000000000000620.
2. Taylor BD, Totten PA, Astete SG, Ferris MJ, Martin DH, Ness RB, Haggerty CL. 2018. Toll-like receptor variants and cervical Atopobium vaginae infection in women with pelvic inflammatory disease. Am J Reprod Immunol 79:e12804. https://doi.org/10.1111/aji.12804.
3. Gómez LM, Sammel MD, Appleby DH, Elovitz MA, Baldwin DA, Jeffcoat MK, Macones GA, Parry S. 2010. Evidence of a gene-environment interaction that predisposes to spontaneous preterm birth: a role for asymptomatic bacterial vaginosis and DNA variants in genes that control the inflammatory response. Am J Obstet Gynecol 202:386.e1–386.e6. https://doi.org/10.1016/j.ajog.2010.01.042.
4. Lamont RF, Sobel JD, Akins RA, Hassan SS, Chaiworapongsa T, Kusanovic JP, Romero R. 2011. The vaginal microbiome: new information about genital tract flora using molecular based techniques. BJOG 118:533–549. https://doi.org/10.1111/j.1471-0528.2010.02840.x.
5. McKinnon LR, Achilles SL, Bradshaw CS, Burgener A, Crucitti T, Fredricks DN, Jaspan HB, Kaul R, Kaushic C, Klatt N, Kwon DS, Marrazzo JM, Masson L, McClelland RS, Ravel J, van de Wijgert JHHM, Vodstrcil LA, Tachedjian G. 2019. The evolving facets of bacterial vaginosis: implications for HIV transmission. AIDS Res Hum Retroviruses 35:219–228. https://doi.org/10.1089/AID.2018.0304.
6. Romero R, Dey SK, Fisher SJ. 2014. Preterm labor: one syndrome, many causes. Science 345:760–765. https://doi.org/10.1126/science.1251816.
7. Molenaar MC, Singer M, Ouburg S. 2018. The two-sided role of the vaginal microbiome in Chlamydia trachomatis and Mycoplasma genitalium pathogenesis. J Reprod Immunol 130:11–17. https://doi.org/10.1016/j.jri.2018.08.006.
8. Huang B, Fettweis JM, Brooks JP, Jefferson KK, Buck GA. 2014. The changing landscape of the vaginal microbiome. Clin Lab Med 34:747–761. https://doi.org/10.1016/j.cll.2014.08.006.
9. Srinivasan S, Morgan MT, Fiedler TL, Djukovic D, Hoffman NG, Raftery D, Marrazzo JM, Fredricks DN. 2015. Metabolic signatures of bacterial vaginosis. mBio 6:e00204-15. https://doi.org/10.1128/mBio.00204-15.
10. Pekmezovic M, Mogavero S, Naglik JR, Hube B. 2019. Host-pathogen interactions during female genital tract infections. Trends Microbiol 27:982–996. https://doi.org/10.1016/j.tim.2019.07.006.
11. Rowley J, Vander Hoorn S, Korenromp E, Low N, Unemo M, Abu-Raddad LJ, Chico RM, Smolak A, Newman L, Gottlieb S, Thwin SS, Broutet N, Taylor MM. 2019. Chlamydia, gonorrhoea, trichomoniasis and syphilis: global prevalence and incidence estimates, 2016. Bull World Health Organ 97:548–562P. https://doi.org/10.2471/BLT.18.228486.
12. Nouioui I, Carro L, García-López M, Meier-Kolthoff JP, Woyke T, Kyrpides NC, Pukall R, Klenk HP, Goodfellow M, Göker M. 2018. Genome-based taxonomic classification of the phylum actinobacteria. Front Microbiol 9:2007. https://doi.org/10.3389/fmicb.2018.02007.
13. Bär A-K, Phukan N, Pinheiro J, Simoes-Barbosa A. 2015. The interplay of host microbiota and parasitic protozoans at mucosal interfaces: implications for the outcomes of infections and diseases. PLoS Negl Trop Dis 9:e0004176. https://doi.org/10.1371/journal.pntd.0004176.
14. Hinderfeld AS, Simoes-Barbosa A. 2020. Vaginal dysbiotic bacteria act as pathobionts of the protozoal pathogen Trichomonas vaginalis. Microb Pathog 138:103820. https://doi.org/10.1016/j.micpath.2019.103820.
15. Fichorova RN, Buck OR, Yamamoto HS, Fashemi T, Dawood HY, Fashemi B, Hayes GR, Beach DH, Takagi Y, Delaney ML, Nibert ML, Singh BN, Onderdonk AB. 2013. The villain team-up or how Trichomonas vaginalis and bacterial vaginosis alter innate immunity in concert. Sex Transm Infect 89:460–466. https://doi.org/10.1136/sextrans-2013-051052.
16. Hinderfeld AS, Phukan N, Bär A-K, Roberton AM, Simoes-Barbosa A. 2019. Cooperative interactions between Trichomonas vaginalis and associated bacteria enhance paracellular permeability of the cervicovaginal epithelium by dysregulating tight junctions. Infect Immun 87:e00141-19. https://doi.org/10.1128/IAI.00141-19.
17. Rappelli P, Addis MF, Carta F, Fiori PL. 1998. Mycoplasma hominis parasitism of Trichomonas vaginalis. Lancet 352:1286. https://doi.org/10.1016/S0140-6736(98)00041-5.
18. Gupta RS, Sawnani S, Adeolu M, Alnajar S, Oren A. 2018. Phylogenetic framework for the phylum Tenericutes based on genome sequence data: proposal for the creation of a new order Mycoplasmoidales ord. nov., containing two new families Mycoplasmoidaceae fam. nov. and Metamycoplasmataceae fam. nov. harbouring Eperythrozoon, Ureaplasma and five novel genera. Antonie Van Leeuwenhoek 111:1583–1630. https://doi.org/10.1007/s10482-018-1047-3.
19. Capoccia R, Greub G, Baud D. 2013. Ureaplasma urealyticum, Mycoplasma hominis and adverse pregnancy outcomes. Curr Opin Infect Dis 26:231–240. https://doi.org/10.1097/QCO.0b013e328360db58.
20. Dessì D, Margarita V, Cocco AR, Marongiu A, Fiori PL, Rappelli P. 2019. Trichomonas vaginalis and Mycoplasma hominis: new tales of two old friends. Parasitology 146:1150–1155. https://doi.org/10.1017/S0031182018002135.
21. Fichorova RN, Fraga J, Rappelli P, Fiori PL. 2017. Trichomonas vaginalis infection in symbiosis with Trichomonasvirus and Mycoplasma. Res Microbiol 168:882–891. https://doi.org/10.1016/j.resmic.2017.03.005.
22. Margarita V, Rappelli P, Dessì D, Pintus G, Hirt RP, Fiori PL. 2016. Symbiotic association with Mycoplasma hominis can influence growth rate, ATP production, cytolysis and inflammatory response of Trichomonas vaginalis. Front Microbiol 7:953. https://doi.org/10.3389/fmicb.2016.00953.
23. Vancini R, Pereira-Neves A, Borojevic R, Benchimol M. 2008. Trichomonas vaginalis harboring Mycoplasma hominis increases cytopathogenicity in vitro. Eur J Clin Microbiol Infect Dis 27:259–267. https://doi.org/10.1007/s10096-007-0422-1.
24. Morada M, Manzur M, Lam B, Tan C, Tachezy J, Rappelli P, Dessì D, Fiori PL, Yarlett N. 2010. Arginine metabolism in Trichomonas vaginalis infected with Mycoplasma hominis. Microbiology (Reading) 156:3734–3743. https://doi.org/10.1099/mic.0.042192-0.
25. Fiori PL, Diaz N, Cocco AR, Rappelli P, Dessi D. 2013. Association of Trichomonas vaginalis with its symbiont Mycoplasma hominis synergistically upregulates the in vitro proinflammatory response of human monocytes. Sex Transm Infect 89:449–454. https://doi.org/10.1136/sextrans-2012-051006.
26. Martin DH, Zozaya M, Lillis RA, Myers L, Nsuami MJ, Ferris MJ. 2013. Unique vaginal microbiota that includes an unknown Mycoplasma-like organism is associated with Trichomonas vaginalis infection. J Infect Dis 207:1922–1931. https://doi.org/10.1093/infdis/jit100.
27. Fettweis JM, Serrano MG, Huang B, Brooks JP, Glascock AL, Sheth NU, Vaginal Microbiome Consortium, Strauss JF, III, Jefferson KK, Buck GA. 2014. An emerging mycoplasma associated with trichomoniasis, vaginal infection and disease. PLoS One 9:e110943. https://doi.org/10.1371/journal.pone.0110943.
28. Costello EK, Carlisle EM, Bik EM, Morowitz MJ, Relman DA. 2013. Microbiome assembly across multiple body sites in low-birthweight infants. mBio 4:e00782-13. https://doi.org/10.1128/mBio.00782-13.
29. Costello EK, Sun CL, Carlisle EM, Morowitz MJ, Banfield JF, Relman DA. 2017. Candidatus Mycoplasma girerdii replicates, diversifies, and co-occurs with Trichomonas vaginalis in the oral cavity of a premature infant. Sci Rep 7:3764. https://doi.org/10.1038/s41598-017-03821-7.
30. Stout MJ, Zhou Y, Wylie KM, Tarr PI, Macones GA, Tuuli MG. 2017. Early pregnancy vaginal microbiome trends and preterm birth. Am J Obstet Gynecol 217:356.e1–356.e18. https://doi.org/10.1016/j.ajog.2017.05.030.
31. Callahan BJ, DiGiulio DB, Goltsman DSA, Sun CL, Costello EK, Jeganathan P, Biggio JR, Wong RJ, Druzin ML, Shaw GM, Stevenson DK, Holmes SP, Relman DA. 2017. Replication and refinement of a vaginal microbial signature of preterm birth in two racially distinct cohorts of US women. Proc Natl Acad Sci U S A 114:9966–9971. https://doi.org/10.1073/pnas.1705899114.
32. Fettweis JM, Serrano MG, Brooks JP, Edwards DJ, Girerd PH, Parikh HI, Huang B, Arodz TJ, Edupuganti L, Glascock AL, Xu J, Jimenez NR, Vivadelli SC, Fong SS, Sheth NU, Jean S, Lee V, Bokhari YA, Lara AM, Mistry SD, Duckworth RA, III, Bradley SP, Koparde VN, Orenda XV, Milton SH, Rozycki SK, Matveyev AV, Wright ML, Huzurbazar SV, Jackson EM, Smirnova E, Korlach J, Tsai Y-C, Dickinson MR, Brooks JL, Drake JI, Chaffin DO, Sexton AL, Gravett MG, Rubens CE, Wijesooriya NR, Hendricks-Muñoz KD, Jefferson KK, Strauss JF, III, Buck GA. 2019. The vaginal microbiome and preterm birth. Nat Med 25:1012–1021. https://doi.org/10.1038/s41591-019-0450-2.
33. Hirt RP, Sherrard J. 2015. Trichomonas vaginalis origins, molecular pathobiology and clinical considerations. Curr Opin Infect Dis 28:72–79. https://doi.org/10.1097/QCO.0000000000000128.
34. Beeson JG, Homer CSE, Morgan C, Menendez C. 2018. Multiple morbidities in pregnancy: time for research, innovation, and action. PLoS Med 15:e1002665. https://doi.org/10.1371/journal.pmed.1002665.
35. Pereyre S, Sirand-Pugnet P, Beven L, Charron A, Renaudin H, Barré A, Avenaud P, Jacob D, Couloux A, Barbe V, de Daruvar A, Blanchard A,

Bébéar C. 2009. Life on arginine for Mycoplasma hominis: clues from its minimal genome and comparison with other human urogenital mycoplasmas. PLoS Genet 5:e1000677. https://doi.org/10.1371/journal.pgen.1000677.
36. Sharma A. 2010. Virulence mechanisms of Tannerella forsythia. Periodontol 2000 54:106–116. https://doi.org/10.1111/j.1600-0757.2009.00332.x.
37. Noël CJ, Diaz N, Sicheritz-Ponten T, Safarikova L, Tachezy J, Tang P, Fiori PL, Hirt RP. 2010. Trichomonas vaginalis vast BspA-like gene family: evidence for functional diversity from structural organisation and transcriptomics. BMC Genomics 11:99. https://doi.org/10.1186/1471-2164-11-99.
38. Onishi S, Honma K, Liang S, Stathopoulou P, Kinane D, Hajishengallis G, Sharma A. 2008. Toll-like receptor 2-mediated interleukin-8 expression in gingival epithelial cells by the Tannerella forsythia leucine-rich repeat protein BspA. Infect Immun 76:198–205. https://doi.org/10.1128/IAI.01139-07.
39. Xu S, Wang Z, Zhou H, Fu Y, Feng M, Cheng X. 2021. High co-infection rate of Trichomonas vaginalis and Candidatus Mycoplasma girerdii in Gansu Province, China. Healthcare (Basel) 9:706. https://doi.org/10.3390/healthcare9060706.
40. Greathouse KL, Sinha R, Vogtmann E. 2019. DNA extraction for human microbiome studies: the issue of standardization. Genome Biol 20:212. https://doi.org/10.1186/s13059-019-1843-8.
41. Demeke T, Jenkins GR. 2010. Influence of DNA extraction methods, PCR inhibitors and quantification methods on real-time PCR assay of biotechnology-derived traits. Anal Bioanal Chem 396:1977–1990. https://doi.org/10.1007/s00216-009-3150-9.
42. van Tongeren SP, Degener JE, Harmsen HJM. 2011. Comparison of three rapid and easy bacterial DNA extraction methods for use with quantitative real-time PCR. Eur J Clin Microbiol Infect Dis 30:1053–1061. https://doi.org/10.1007/s10096-011-1191-4.
43. Elsinghorst EA. 1994. Measurement of invasion by gentamicin resistance. Methods Enzymol 236:405–420. https://doi.org/10.1016/0076-6879(94)36030-8.
44. Vancini RG, Benchimol M. 2008. Entry and intracellular location of Mycoplasma hominis in Trichomonas vaginalis. Arch Microbiol 189:7–18. https://doi.org/10.1007/s00203-007-0288-8.
45. Dessì D, Delogu G, Emonte E, Catania R, Fiori PL, Rappelli P. 2005. Long-term survival and intracellular replication of Mycoplasma hominis in Trichomonas vaginalis cells: potential role of the protozoon in transmitting bacterial infection. Infect Immun 73:1180–1186. https://doi.org/10.1128/IAI.73.2.1180-1186.2005.
46. Carlton JM, Hirt RP, Silva JC, Delcher AL, Schatz M, Zhao Q, Wortman JR, Bidwell SL, Alsmark UCM, Besteiro S, Sicheritz-Ponten T, Noel CJ, Dacks JB, Foster PG, Simillion C, Van de Peer Y, Miranda-Saavedra D, Barton GJ, Westrop GD, Müller S, Dessi D, Fiori PL, Ren Q, Paulsen I, Zhang H, Bastida-Corcuera FD, Simoes-Barbosa A, Brown MT, Hayes RD, Mukherjee M, Okumura CY, Schneider R, Smith AJ, Vanacova S, Villalvazo M, Haas BJ, Pertea M, Feldblyum TV, Utterback TR, Shu C-L, Osoegawa K, de Jong PJ, Hrdy I, Horvathova L, Zubacova Z, Dolezal P, Malik S-B, Logsdon JM, Jr, Henze K, Gupta A, et al. 2007. Draft genome sequence of the sexually transmitted pathogen Trichomonas vaginalis. Science 315:207–212. https://doi.org/10.1126/science.1132894.
47. Rappelli P, Carta F, Delogu G, Addis MF, Dessì D, Cappuccinelli P, Fiori PL. 2001. Mycoplasma hominis and Trichomonas vaginalis symbiosis: multiplicity of infection and transmissibility of M. hominis to human cells. Arch Microbiol 175:70–74. https://doi.org/10.1007/s002030000240.
48. Fürnkranz U, Henrich B, Walochnik J. 2018. Mycoplasma hominis impacts gene expression in Trichomonas vaginalis. Parasitol Res 117:841–847. https://doi.org/10.1007/s00436-018-5761-6.
49. Wu G, Fiser A, ter Kuile B, Sali A, Müller M. 1999. Convergent evolution of Trichomonas vaginalis lactate dehydrogenase from malate dehydrogenase. Proc Natl Acad Sci U S A 96:6285–6290. https://doi.org/10.1073/pnas.96.11.6285.
50. Bologna FP, Andreo CS, Drincovich MF. 2007. Escherichia coli malic enzymes: two isoforms with substantial differences in kinetic properties, metabolic regulation, and structure. J Bacteriol 189:5937–5946. https://doi.org/10.1128/JB.00428-07.
51. Burstein D, Gould SB, Zimorski V, Kloesges T, Kiosse F, Major P, Martin WF, Pupko T, Dagan T. 2012. A machine learning approach to identify hydrogenosomal proteins in Trichomonas vaginalis. Eukaryot Cell 11:217–228. https://doi.org/10.1128/EC.05225-11.
52. Sankaranarayanan R, Cherney MM, Cherney LT, Garen CR, Moradian F, James MNG. 2008. The crystal structures of ornithine carbamoyltransferase from Mycobacterium tuberculosis and its ternary complex with carbamoyl phosphate and L-norvaline reveal the enzyme's catalytic mechanism. J Mol Biol 375:1052–1063. https://doi.org/10.1016/j.jmb.2007.11.025.
53. Handrich MR, Garg SG, Sommerville EW, Hirt RP, Gould SB. 2019. Characterization of the BspA and Pmp protein family of trichomonads. Parasit Vectors 12:406. https://doi.org/10.1186/s13071-019-3660-z.
54. de Miguel N, Lustig G, Twu O, Chattopadhyay A, Wohlschlegel JA, Johnson PJ. 2010. Proteome analysis of the surface of Trichomonas vaginalis reveals novel proteins and strain-dependent differential expression. Mol Cell Proteomics 9:1554–1566. https://doi.org/10.1074/mcp.M000022-MCP201.
55. Twu O, de Miguel N, Lustig G, Stevens GC, Vashisht AA, Wohlschlegel JA, Johnson PJ. 2013. Trichomonas vaginalis exosomes deliver cargo to host cells and mediate host:parasite interactions. PLoS Pathog 9:e1003482. https://doi.org/10.1371/journal.ppat.1003482.
56. Olmos-Ortiz LM, Barajas-Mendiola MA, Barrios-Rodiles M, Castellano LE, Arias-Negrete S, Avila EE, Cuéllar-Mata P. 2017. Trichomonas vaginalis exosome-like vesicles modify the cytokine profile and reduce inflammation in parasite-infected mice. Parasite Immunol 39:e12426. https://doi.org/10.1111/pim.12426.
57. Hirt RP, de Miguel N, Nakjang S, Dessì D, Liu YC, Diaz N, Rappelli P, Acosta-Serrano A, Fiori PL, Mottram JC. 2011. Trichomonas vaginalis pathobiology. New insights from the genome sequence. Adv Parasitol 77:87–140. https://doi.org/10.1016/B978-0-12-391429-3.00006-X.
58. Lasa I, Penadés JR. 2006. Bap: a family of surface proteins involved in biofilm formation. Res Microbiol 157:99–107. https://doi.org/10.1016/j.resmic.2005.11.003.
59. Ebbes M, Bleymüller WM, Cernescu M, Nölker R, Brutschy B, Niemann HH. 2011. Fold and function of the InlB B-repeat. J Biol Chem 286:15496–15506. https://doi.org/10.1074/jbc.M110.189951.
60. Fiori PL, Rappelli P, Rocchigiani AM, Cappuccinelli P. 1993. Trichomonas vaginalis haemolysis: evidence of functional pores formation on red cell membranes. FEMS Microbiol Lett 109:13–18. https://doi.org/10.1111/j.1574-6968.1993.tb06136.x.
61. Margarita V, Fiori PL, Rappelli P. 2020. Impact of symbiosis between Trichomonas vaginalis and Mycoplasma hominis on vaginal dysbiosis: a mini review. Front Cell Infect Microbiol 10:179. https://doi.org/10.3389/fcimb.2020.00179.
62. Thu TTT, Margarita V, Cocco AR, Marongiu A, Dessì D, Rappelli P, Fiori PL. 2018. Trichomonas vaginalis transports virulent Mycoplasma hominis and transmits the infection to human cells after metronidazole treatment: a potential role in bacterial invasion of fetal membranes and amniotic fluid. J Pregnancy 2018:5037181. https://doi.org/10.1155/2018/5037181.
63. Fichorova RN, Lee Y, Yamamoto HS, Takagi Y, Hayes GR, Goodman RP, Chepa-Lotrea X, Buck OR, Murray R, Kula T, Beach DH, Singh BN, Nibert ML. 2012. Endobiont viruses sensed by the human host—beyond conventional antiparasitic therapy. PLoS One 7:e48418. https://doi.org/10.1371/journal.pone.0048418.
64. Brotman RM, Bradford LL, Conrad M, Gajer P, Ault K, Peralta L, Forney LJ, Carlton JM, Abdo Z, Ravel J. 2012. Association between Trichomonas vaginalis and vaginal bacterial community composition among reproductive-age women. Sex Transm Dis 39:807–812. https://doi.org/10.1097/OLQ.0b013e3182631c79.
65. McLaren MR, Willis AD, Callahan BJ. 2019. Consistent and correctable bias in metagenomic sequencing experiments. Elife 8:e46923. https://doi.org/10.7554/eLife.46923.
66. Huang KY, Ong SC, Wu CC, Hsu CW, Lin HC, Fang YK, Cheng WH, Huang PJ, Chiu CH, Tang P. 2019. Metabolic reprogramming of hydrogenosomal amino acids in Trichomonas vaginalis under glucose restriction. J Microbiol Immunol Infect 52:630–637. https://doi.org/10.1016/j.jmii.2017.10.005.
67. Kulda J. 1999. Trichomonads, hydrogenosomes and drug resistance. Int J Parasitol 29:199–212. https://doi.org/10.1016/s0020-7519(98)00155-6.
68. Westrop GD, Wang L, Blackburn GJ, Zhang T, Zheng L, Watson DG, Coombs GH. 2017. Metabolomic profiling and stable isotope labelling of Trichomonas vaginalis and Tritrichomonas foetus reveal major differences in amino acid metabolism including the production of 2-hydroxyisocaproic acid, cystathionine and S-methylcysteine. PLoS One 12:e0189072. https://doi.org/10.1371/journal.pone.0189072.
69. Linstead D, Cranshaw MA. 1983. The pathway of arginine catabolism in the parasitic flagellate Trichomonas vaginalis. Mol Biochem Parasitol 8:241–252. https://doi.org/10.1016/0166-6851(83)90046-4.
70. Garcia AF, Benchimol M, Alderete JF. 2005. Trichomonas vaginalis polyamine metabolism is linked to host cell adherence and cytotoxicity. Infect Immun 73:2602–2610. https://doi.org/10.1128/IAI.73.5.2602-2610.2005.

71. Phillips MA. 2018. Polyamines in protozoan pathogens. J Biol Chem 293:18746–18756. https://doi.org/10.1074/jbc.TM118.003342.
72. Brauer MJ, Huttenhower C, Airoldi EM, Rosenstein R, Matese JC, Gresham D, Boer VM, Troyanskaya OG, Botstein D. 2008. Coordination of growth rate, cell cycle, stress response, and metabolic activity in yeast. Mol Biol Cell 19:352–367. https://doi.org/10.1091/mbc.e07-08-0779.
73. Hopfe M, Deenen R, Degrandi D, Köhrer K, Henrich B. 2013. Host cell responses to persistent mycoplasmas—different stages in infection of HeLa cells with Mycoplasma hominis. PLoS One 8:e54219. https://doi.org/10.1371/journal.pone.0054219.
74. McMullen JG, II, Peterson BF, Forst S, Blair HG, Stock SP. 2017. Fitness costs of symbiont switching using entomopathogenic nematodes as a model. BMC Evol Biol 17:100. https://doi.org/10.1186/s12862-017-0939-6.
75. Mercer F, Diala FGI, Chen Y-P, Molgora BM, Ng SH, Johnson PJ. 2016. Leukocyte lysis and cytokine induction by the human sexually transmitted parasite Trichomonas vaginalis. PLoS Negl Trop Dis 10:e0004913. https://doi.org/10.1371/journal.pntd.0004913.
76. Pereira-Neves A, Benchimol M. 2007. Phagocytosis by Trichomonas vaginalis: new insights. Biol Cell 99:87–101. https://doi.org/10.1042/BC20060084.
77. Rendón-Maldonado JG, Espinosa-Cantellano M, González-Robles A, Martínez-Palomo A. 1998. Trichomonas vaginalis: in vitro phagocytosis of lactobacilli, vaginal epithelial cells, leukocytes, and erythrocytes. Exp Parasitol 89:241–250. https://doi.org/10.1006/expr.1998.4297.
78. Li H, Zhou X, Huang Y, Liao B, Cheng L, Ren B. 2021. Reactive oxygen species in pathogen clearance: the killing mechanisms, the adaption response, and the side effects. Front Microbiol 11:622534. https://doi.org/10.3389/fmicb.2020.622534.
79. Fettweis JM, Serrano MG, Sheth NU, Mayer CM, Glascock AL, Brooks JP, Jefferson KK, Vaginal Microbiome Consortium (additional members), Buck GA. 2012. Species-level classification of the vaginal microbiome. BMC Genomics 13(Suppl 8):S17. https://doi.org/10.1186/1471-2164-13-S8-S17.
80. Clark CG, Diamond LS. 2002. Methods for cultivation of luminal parasitic protists of clinical importance. Clin Microbiol Rev 15:329–341. https://doi.org/10.1128/CMR.15.3.329-341.2002.
81. Andersen H, Birkelund S, Christiansen G, Freundt EA. 1987. Electrophoretic analysis of proteins from Mycoplasma hominis strains detected by SDS-PAGE, two-dimensional gel electrophoresis and immunoblotting. J Gen Microbiol 133:181–191. https://doi.org/10.1099/00221287-133-1-181.
82. Cacciotto C, Dessì D, Cubeddu T, Cocco AR, Pisano A, Tore G, Fiori PL, Rappelli P, Pittau M, Alberti A. 2019. MHO_0730 as a surface-exposed calcium-dependent nuclease of Mycoplasma hominis promoting neutrophil extracellular trap formation and escape. J Infect Dis 220:1999–2008. https://doi.org/10.1093/infdis/jiz406.
83. Leinonen R, Sugawara H, Shumway M, International Nucleotide Sequence Database Collaboration. 2011. The Sequence Read Archive. Nucleic Acids Res 39:D19–D21. https://doi.org/10.1093/nar/gkq1019.
84. Dobin A, Davis CA, Schlesinger F, Drenkow J, Zaleski C, Jha S, Batut P, Chaisson M, Gingeras TR. 2013. STAR: ultrafast universal RNA-seq aligner. Bioinformatics 29:15–21. https://doi.org/10.1093/bioinformatics/bts635.
85. Shen W, Xiong J. 2019. TaxonKit: a cross-platform and efficient NCBI taxonomy toolkit. bioRxiv 513523.
86. O'Leary NA, Wright MW, Brister JR, Ciufo S, Haddad D, McVeigh R, Rajput B, Robbertse B, Smith-White B, Ako-Adjei D, Astashyn A, Badretdin A, Bao Y, Blinkova O, Brover V, Chetvernin V, Choi J, Cox E, Ermolaeva O, Farrell CM, Goldfarb T, Gupta T, Haft D, Hatcher E, Hlavina W, Joardar VS, Kodali VK, Li W, Maglott D, Masterson P, McGarvey KM, Murphy MR, O'Neill K, Pujar S, Rangwala SH, Rausch D, Riddick LD, Schoch C, Shkeda A, Storz SS, Sun H, Thibaud-Nissen F, Tolstoy I, Tully RE, Vatsan AR, Wallin C, Webb D, Wu W, Landrum MJ, Kimchi A, et al. 2016. Reference Sequence (RefSeq) database at NCBI: current status, taxonomic expansion, and functional annotation. Nucleic Acids Res 44:D733–D745. https://doi.org/10.1093/nar/gkv1189.
87. Li H, Handsaker B, Wysoker A, Fennell T, Ruan J, Homer N, Marth G, Abecasis G, Durbin R, 1000 Genome Project Data Processing Subgroup. 2009. The Sequence Alignment/Map format and SAMtools. Bioinformatics 25:2078–2079. https://doi.org/10.1093/bioinformatics/btp352.
88. Narasimhan V, Danecek P, Scally A, Xue Y, Tyler-Smith C, Durbin R. 2016. BCFtools/RoH: a hidden Markov model approach for detecting autozygosity from next-generation sequencing data. Bioinformatics 32:1749–1751. https://doi.org/10.1093/bioinformatics/btw044.
89. Danecek P, Auton A, Abecasis G, Albers CA, Banks E, DePristo MA, Handsaker RE, Lunter G, Marth GT, Sherry ST, McVean G, Durbin R, 1000 Genomes Project Analysis Group. 2011. The variant call format and VCFtools. Bioinformatics 27:2156–2158. https://doi.org/10.1093/bioinformatics/btr330.
90. Bushmanova E, Antipov D, Lapidus A, Prjibelski AD. 2019. rnaSPAdes: a de novo transcriptome assembler and its application to RNA-Seq data. Gigascience 8:giz100. https://doi.org/10.1093/gigascience/giz100.
91. Robinson MD, Oshlack A. 2010. A scaling normalization method for differential expression analysis of RNA-seq data. Genome Biol 11:R25. https://doi.org/10.1186/gb-2010-11-3-r25.
92. Robinson MD, McCarthy DJ, Smyth GK. 2010. edgeR: a Bioconductor package for differential expression analysis of digital gene expression data. Bioinformatics 26:139–140. https://doi.org/10.1093/bioinformatics/btp616.
93. Thomas PD, Campbell MJ, Kejariwal A, Mi H, Karlak B, Daverman R, Diemer K, Muruganujan A, Narechania A. 2003. PANTHER: a library of protein families and subfamilies indexed by function. Genome Res 13:2129–2141. https://doi.org/10.1101/gr.772403.
94. Wu D, Lim E, Vaillant F, Asselin-Labat M-L, Visvader JE, Smyth GK. 2010. ROAST: rotation gene set tests for complex microarray experiments. Bioinformatics 26:2176–2182. https://doi.org/10.1093/bioinformatics/btq401.
95. Sun L, Dong S, Ge Y, Fonseca JP, Robinson ZT, Mysore KS, Mehta P. 2019. DiVenn: an interactive and integrated Web-based visualization tool for comparing gene lists. Front Genet 10:421. https://doi.org/10.3389/fgene.2019.00421.
96. Kanehisa M, Sato Y, Kawashima M, Furumichi M, Tanabe M. 2016. KEGG as a reference resource for gene and protein annotation. Nucleic Acids Res 44:D457–D462. https://doi.org/10.1093/nar/gkv1070.
97. Jones P, Binns D, Chang H-Y, Fraser M, Li W, McAnulla C, McWilliam H, Maslen J, Mitchell A, Nuka G, Pesseat S, Quinn AF, Sangrador-Vegas A, Scheremetjew M, Yong S-Y, Lopez R, Hunter S. 2014. InterProScan 5: genome-scale protein function classification. Bioinformatics 30:1236–1240. https://doi.org/10.1093/bioinformatics/btu031.
98. Lustig G, Ryan CM, Secor WE, Johnson PJ. 2013. Trichomonas vaginalis contact-dependent cytolysis of epithelial cells. Infect Immun 81:1411–1419. https://doi.org/10.1128/IAI.01244-12.
99. Yang R, Klimentová J, Göckel-Krzikalla E, Ly R, Gmelin N, Hotz-Wagenblatt A, Řehulková H, Stulík J, Rösl F, Niebler M. 2019. Combined transcriptome and proteome analysis of immortalized human keratinocytes expressing human papillomavirus 16 (HPV16) oncogenes reveals novel key factors and networks in HPV-induced carcinogenesis. mSphere 4:e00129-19. https://doi.org/10.1128/mSphere.00129-19.
100. R Core Team. 2018. R: a language and environment for statistical computing. R Foundation for Statistical Computing, Vienna, Austria. https://www.R-project.org.